

MIT OpenCourseWare

<http://ocw.mit.edu>

Electromechanical Dynamics

For any use or distribution of this textbook, please cite as follows:

Woodson, Herbert H., and James R. Melcher. *Electromechanical Dynamics*. 3 vols. (Massachusetts Institute of Technology: MIT OpenCourseWare). <http://ocw.mit.edu> (accessed MM DD, YYYY). License: Creative Commons Attribution-NonCommercial-Share Alike

For more information about citing these materials or our Terms of Use, visit: <http://ocw.mit.edu/terms>

Chapter 11

INTRODUCTION TO THE ELECTROMECHANICS OF ELASTIC MEDIA

11.0 INTRODUCTION

Most electromechanical effects and devices involving deformable solid media are best understood in terms of specific models. Elastic membranes and wires are examples of simple one-dimensional and two-dimensional models that can be developed without recourse to a more general theory of elasticity*. Any particular analysis can be developed in this way, and if our objective were to understand specific examples this would be our approach. A more general description of elastic media serves the purpose of giving a larger picture, with the specific examples placed in perspective. Our objective in this chapter is this larger picture. At the same time, examples which emphasize that special models still play an essential role are developed from the general theory.

The material of this chapter is, of course, relevant to the dynamics of a variety of electromechanical interactions with elastic solids. In particular, it relates to areas of electromechanics such as physical acoustics, the microwave electromechanics of crystals, and the development of electromechanical distributed circuits.

The one-dimensional example of a rod subject to longitudinal motions introduced in Section 9.1* illustrates the essential steps required to find the equations of motion for an elastic continuum. First, an equation expressing force equilibrium for a small volume of material is written in terms of the material displacement and the mechanical stresses. Then the stresses are related to the strain, hence to the displacement, by means of the stress-strain relations. The first step, which can be completed without regard to the

* See Chapter 9 or Table 9.2, Appendix G.

elastic properties of the material, is given in the next section. The second step, for isotropic media, is found in Section 11.2. In Section 11.5 we introduce enough of the properties of anisotropic materials to consider certain illustrative examples.

11.1 FORCE EQUILIBRIUM

Our first objective is to write an equation that expresses force equilibrium for an element of material. A small cube of the material, centered at (x_1, x_2, x_3) , is shown in Fig. 11.1.1. To write Newton's law we must know the instantaneous acceleration of the material at this point. The particles of matter found at (x_1, x_2, x_3) have a displacement from their unstressed position given by

$$\delta(x_1 - \delta_1, x_2 - \delta_2, x_3 - \delta_3, t). \quad (11.1.1)$$

This is true because $\delta(a, b, c, t)$ is defined as the displacement of the particle with an unstressed position (a, b, c) .* As pointed out in Section 9.1, displacements are small in many important situations. If we limit ourselves to small displacements, (11.1.1) can be expanded about the position (x_1, x_2, x_3) to give

$$\begin{aligned} &\delta(x_1 - \delta_1, x_2 - \delta_2, x_3 - \delta_3, t) \\ &= \delta(x_1, x_2, x_3, t) - \frac{\partial \delta}{\partial x_1} \delta_1 - \frac{\partial \delta}{\partial x_2} \delta_2 - \frac{\partial \delta}{\partial x_3} \delta_3 + \dots \end{aligned} \quad (11.1.2)$$

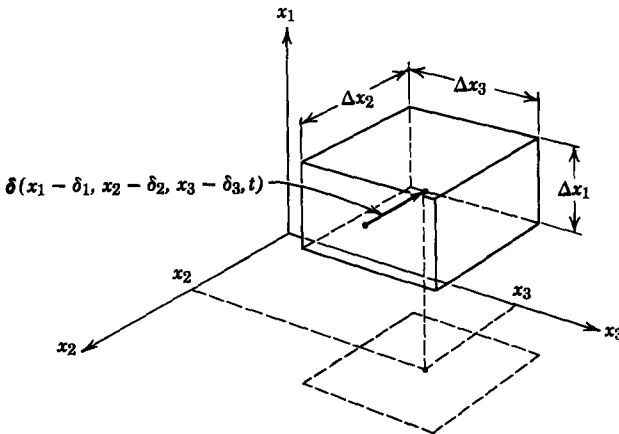


Fig. 11.1.1 Element of material with volume V centered at the position (x_1, x_2, x_3) . The grain of material at the center of the cube has the unstressed position $(x_1 - \delta_1, x_2 - \delta_2, x_3 - \delta_3)$.

* A function such as δ , which follows the motion of a particular particle, is said to be written in Lagrangian coordinates. The coordinates indicate the particle under consideration.

If the displacement and its derivatives are small, we can approximate the displacement of the material at the center of the element (Fig. 11.1.1) by the first term on the right, which is the displacement evaluated at the center of the element. Newton's law for the small cube of Fig. 11.1.1 is then

$$\rho \frac{\partial^2 \delta}{\partial t^2} = \mathbf{F}. \quad (11.1.3)$$

Because we ignore products of perturbation quantities, the mass density ρ is a constant in this expression. In an elastic solid there is always a force density \mathbf{F} due to mechanical stresses imposed on the cube by the surrounding material. In the presence of electric or magnetic fields an additional contribution to \mathbf{F} is made by forces of electrical origin. In the next section we develop the relation between elastic stresses and the displacement δ (for homogeneous media) as a stress tensor, and in Chapter 8 it was found that forces due to free charges or free currents could be written as the divergence of a stress tensor*. Hence we can write (11.1.3) as

$$\rho \frac{\partial^2 \delta_m}{\partial t^2} = \frac{\partial T_{mn}}{\partial x_n}, \quad (11.1.4)$$

where it is understood that the stress tensor T_{mn} is due to mechanical (elastic) interactions and (if they are present in the problem) electrical interactions.

11.2 EQUATIONS OF MOTION FOR ISOTROPIC MEDIA

From (11.1.4) it is apparent that to formulate the equations of motion for an elastic medium it is necessary to make a connection between the applied stresses and the resulting deformations. It was shown in Section 9.1 that for a simple, one-dimensional problem this could be done by introducing the strain, which has a simple relationship both with the deformation of the material and the applied stresses. In the section that follows we consider how the strain gives a description of material deformation, hence the relation between the strain and the displacement of the material. Then in Section 11.2.2 a description is given of the relation between the stress and strain.

11.2.1 Strain-Displacement Relations

Two types of material deformation corresponding to the action of normal and shear stresses on the material, are possible. These are illustrated two-dimensionally in Fig. 11.2.1, in which the points A , B , and C represent tagged grains of material that, when strained, move from A to A' , B to B' , and C to C' . Note that in the unstrained condition the lines joining the tagged points are parallel to the coordinate axes. Because the effects considered are linear,

* See Sec. 8.2 or Appendix G.

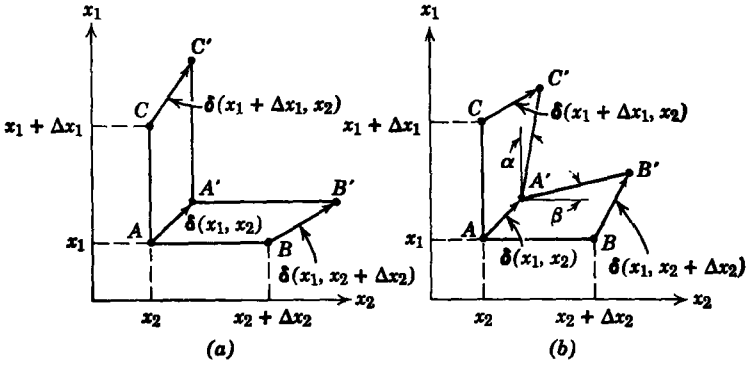


Fig. 11.2.1 (a) Strain produced by normal stresses; (b) strain produced by shear stresses.

the deformations can be considered separately and then superimposed. We shall shortly develop the strain from a formal point of view, and this will make the superposition principle more apparent. At first our development is more intuitive.

In Fig. 11.2.1a the deformation has lengthened the distances AB and AC to the distances $A'B'$ and $A'C'$, whereas in Fig. 11.2.1b these lengths have remained constant but the angles between the sides of the cube of material have changed. The first of the two types of deformation is a generalization of the kind of strain considered in Section 9.1 (the thin elastic rod); that is, we can *define* a normal strain in each of the axis directions as an elongation per unit length. In the x_1 -direction this is

$$e_{11} = \lim_{\Delta x_1 \rightarrow 0} \frac{\delta_1(x_1 + \Delta x_1, x_2) - \delta_1(x_1, x_2)}{\Delta x_1} = \frac{\partial \delta_1}{\partial x_1}, \tag{11.2.1}$$

where $\delta(x_1, x_2, x_3, t)$ is the material displacement at the point x_1, x_2, x_3 , as discussed in Section 11.1. Similarly,

$$e_{22} = \frac{\partial \delta_2}{\partial x_2}, \tag{11.2.2}$$

$$e_{33} = \frac{\partial \delta_3}{\partial x_3}. \tag{11.2.3}$$

In the second kind of deformation (Fig. 11.2.1b) the sides of the cube keep their original length but are deflected with respect to each other to an angle different from the original 90° . This strain is caused by the shear stresses (T_{12}, T_{31} , etc.) and can be visualized by placing the covers of a book under shear, as shown in Fig. 11.2.2. (The significance of the stress components is discussed in Section 8.2 and Appendix G.)

The shear-strains, like the normal strains, are *defined* functions. They are defined as one half the tangent of the change in angle between the originally perpendicular sides of the cube (Fig. 11.2.1b) in the limit in which the cube becomes very small. Hence in the diagram of Fig. 11.2.1b the strain resulting from a change in angle with respect to the x_1 and x_2 axes is designated e_{12} .

In terms of the angles defined in Fig. 11.2.1b the strain e_{12} is

$$e_{12} = \lim_{\substack{\Delta x_1 \rightarrow 0 \\ \Delta x_2 \rightarrow 0}} \frac{1}{2} \tan [\alpha + \beta] \quad (11.2.4)$$

Note that a positive shear strain signifies that the angle between the originally perpendicular lines is less than 90° .

In Chapter 9, Example 9.1.1 was used to illustrate that the deformations commonly encountered in elastic solids are very small. For this reason the angles of deflection due to shear stresses are also commonly small and the tangent function in (11.2.4) can be approximated by the argument $(\alpha + \beta)$. For the same reason the angles α and β can in turn be approximated by their tangents to write

$$\begin{aligned} \alpha &\approx \frac{[\delta_2(x_1 + \Delta x_1, x_2) - \delta_2(x_1, x_2)]}{\Delta x_1}, \\ \beta &\approx \frac{[\delta_1(x_1, x_2 + \Delta x_2) - \delta_1(x_1, x_2)]}{\Delta x_2}, \end{aligned} \quad (11.2.5)$$

(11.2.4) then becomes

$$e_{12} = \lim_{\substack{\Delta x_1 \rightarrow 0 \\ \Delta x_2 \rightarrow 0}} \frac{1}{2} \left\{ \frac{[\delta_2(x_1 + \Delta x_1, x_2) - \delta_2(x_1, x_2)]}{\Delta x_1} + \frac{[\delta_1(x_1, x_2 + \Delta x_2) - \delta_1(x_1, x_2)]}{\Delta x_2} \right\}, \quad (11.2.6)$$

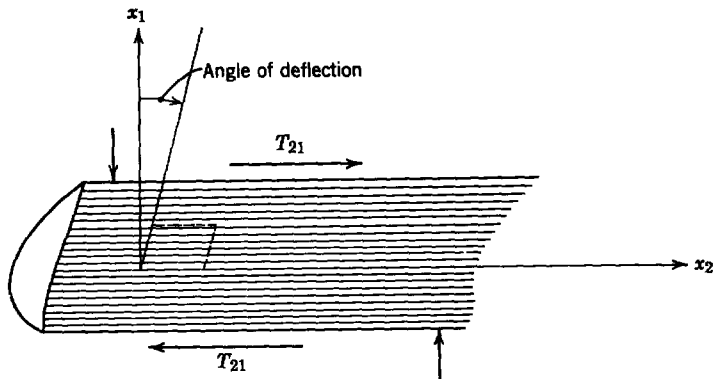


Fig. 11.2.2 Simple situation in which shear stresses result in a shear strain (the angle of deflection).

and in the limit we obtain a point relation between the component of strain e_{12} and the displacements:

$$e_{12} = \frac{1}{2} \left(\frac{\partial \delta_1}{\partial x_2} + \frac{\partial \delta_2}{\partial x_1} \right); \quad (11.2.7)$$

that is, e_{12} is evaluated at the unstressed position A . In the process of taking the limit in which $\Delta x_1 \rightarrow 0$ and $\Delta x_2 \rightarrow 0$ all of the approximations in going from (11.2.4) to (11.2.7) become exact except the one requiring small angular deflections, which remains the basic limitation of the theory.

A two-dimensional picture of shear strain has been used so far because it is easily visualized. A three-dimensional description of the strain follows by considering the deflections between the other two pairs of axes, with the results

$$e_{13} = \frac{1}{2} \left(\frac{\partial \delta_1}{\partial x_3} + \frac{\partial \delta_3}{\partial x_1} \right), \quad (11.2.8)$$

$$e_{23} = \frac{1}{2} \left(\frac{\partial \delta_2}{\partial x_3} + \frac{\partial \delta_3}{\partial x_2} \right). \quad (11.2.9)$$

The last three expressions make it evident that $e_{ij} = e_{ji}$, as would be expected from the definition of the shear strain. Altogether, we have defined nine components of the strain, which are presumably sufficient to describe the distortions of the material in the vicinity of a point x_1, x_2, x_3 related to the stress. We can summarize all the strain components with the expression

$$e_{ij} = \frac{1}{2} \left(\frac{\partial \delta_i}{\partial x_j} + \frac{\partial \delta_j}{\partial x_i} \right). \quad (11.2.10)$$

Note that e_{ij} is a Lagrangian variable in that it is evaluated at the unstressed position of a grain of material (A in Fig. 11.2.1). As discussed in Section 11.1, because the deflections are small it will not be necessary to distinguish between the strain evaluated at the unstressed position of the material and the strain evaluated at the stressed position of the material.

11.2.1a A Formal Derivation

Our remarks about the strain have so far been aimed at establishing the physical significance of each of the nine components. We have not shown in a formal way that the components e_{ij} are sufficient to describe the relative distortions of the material caused by the stresses (although e_{ij} does include all possible space derivatives of δ). To do so we must consider a general material deformation rather than the two particular forms shown in Fig. 11.2.1. The reasoning used now parallels that of the preceding discussion in that we again consider the relative positions of grains of matter.

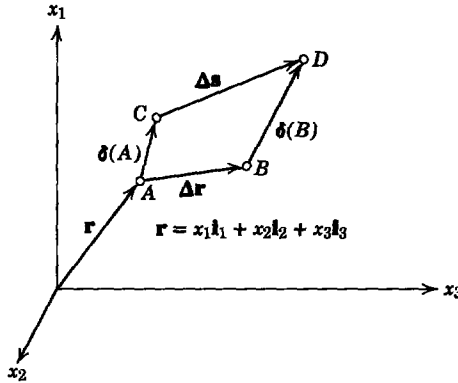


Fig. 11.2.3 Displacement of grains of matter in the unstressed positions A and B and final separation Δs .

Figure 11.2.3 shows two grains of material in the unstrained positions A and B . When the material is subjected to stress, these grains move to the new positions C and D . We are interested in that part of the material distortion that is produced by the stress. Hence we are not interested (when we define the strain) in a uniform translation of the material, or, as we shall see momentarily, we are not interested in uniform rotations of the material. The strain is defined to describe the stretching of the material between the points A and B ; hence attention is given to the distance between the points originally at A and B , as they are distorted to points C and D . At first the relative displacement is $\Delta \mathbf{r}$, whereas after the stress is applied the relative displacement is $\Delta \mathbf{s}$, as shown in Fig. 11.2.3.

The coordinate of the material at A is \mathbf{r} . By taking $\Delta \mathbf{r}$ ($\Delta \mathbf{r} = \Delta x_1 \mathbf{i}_1 + \Delta x_2 \mathbf{i}_2 + \Delta x_3 \mathbf{i}_3$) to be small it is possible to find the separation $\Delta \mathbf{s}$ between the points in the strained positions C and D . First, vector addition of the displacement components shown in Fig. 11.2.3 gives

$$\Delta \mathbf{s} = \Delta \mathbf{r} + \delta(B) - \delta(A), \quad (11.2.11)$$

which becomes approximately (writing the i th component)*

$$\begin{aligned} \Delta s_i &= \Delta x_i + \delta_i(x_1 + \Delta x_1, x_2 + \Delta x_2, x_3 + \Delta x_3, t) - \delta_i(x_1, x_2, x_3, t) \\ &\cong \Delta x_i + \frac{\partial \delta_i}{\partial x_1} \Delta x_1 + \frac{\partial \delta_i}{\partial x_2} \Delta x_2 + \frac{\partial \delta_i}{\partial x_3} \Delta x_3 \\ &\equiv \Delta x_i + \frac{\partial \delta_i}{\partial x_k} \Delta x_k. \end{aligned} \quad (11.2.12)$$

* See Appendix G for index notation.

Now, if the quantity $\frac{1}{2}(\partial\delta_k/\partial x_i) \Delta x_k$ is both added to and subtracted from this equation, we obtain

$$\Delta s_i = \Delta x_i + \frac{1}{2} \left(\frac{\partial\delta_i}{\partial x_k} - \frac{\partial\delta_k}{\partial x_i} \right) \Delta x_k + \frac{1}{2} \left(\frac{\partial\delta_i}{\partial x_k} + \frac{\partial\delta_k}{\partial x_i} \right) \Delta x_k. \quad (11.2.13)$$

Here we have an expression for the i th component of the directed distance $\Delta \mathbf{s}$ between the points A and B after the material has been subjected to stress. This distance is written as a function of the initial distance $\Delta \mathbf{r}$ and the displacement δ of the material in the vicinity of A . Note that in (11.2.13) the derivatives of δ are evaluated at the unstressed position A .

In writing (11.2.13), we have divided the expression for the relative positions of A and B into a part that is due to a pure (rigid body) rotation of the material in the vicinity of A and a part resulting because of the material distortions produced by the applied stress. We have already agreed that a pure translation, and similarly a pure rotation, involve no strain deformation in the material. The bracketed part of the second term on the right in (11.2.13) is one component of the vector $\nabla \times \delta$. Hence it describes a rotation of the material about the unstressed position A . This may be verified by defining a rotation vector Ω in terms of the components of δ .

$$\Omega = \frac{1}{2} \left(\frac{\partial\delta_3}{\partial x_2} - \frac{\partial\delta_2}{\partial x_3} \right) \mathbf{i}_1 + \frac{1}{2} \left(\frac{\partial\delta_1}{\partial x_3} - \frac{\partial\delta_3}{\partial x_1} \right) \mathbf{i}_2 + \frac{1}{2} \left(\frac{\partial\delta_2}{\partial x_1} - \frac{\partial\delta_1}{\partial x_2} \right) \mathbf{i}_3. \quad (11.2.14)$$

Then the second term in (11.2.13) can be written in terms of Ω as

$$\frac{1}{2} \left(\frac{\partial\delta_i}{\partial x_k} - \frac{\partial\delta_k}{\partial x_i} \right) \Delta x_k = (\Omega \times \Delta \mathbf{r})_i. \quad (11.2.15)$$

This is not obvious unless one substitutes (11.2.14) into (11.2.15).

Without specifying the direction of Ω , we can conclude from (11.2.15) that since $\Omega \times \Delta \mathbf{r}$ is perpendicular to $\Delta \mathbf{r}$ the relative displacement represented by this term is also perpendicular to $\Delta \mathbf{r}$. In Fig. 11.2.4 the stressed and unstressed positions of the material are shown in the case in which the contribution of the last term in (11.2.13) is zero. The material initially at points A and B undergoes a uniform translation and then, because Ω is perpendicular to $\Delta \mathbf{r}$, a rigid body rotation.

It is apparently the last term in (11.2.13) that represents a distortion of the material and therefore should be defined as the strain. This is, of course, consistent with our definition of the strain e_{ij} in the preceding section (11.2.10). In view of this definition, (11.2.13) provides an expression for the relative positions of two material particles with the initial relative positions $\Delta \mathbf{r}$.

$$\Delta s_i = \Delta x_i + (\Omega \times \Delta \mathbf{r})_i + e_{ij} \Delta x_j. \quad (11.2.16)$$

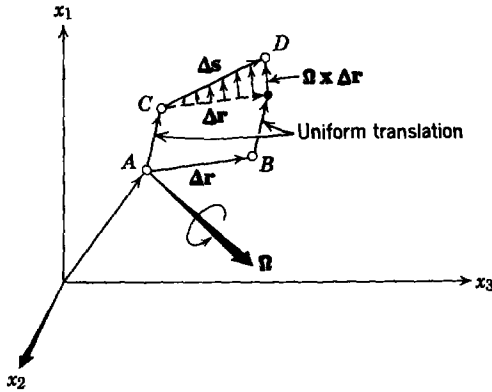


Fig. 11.2.4 Displacements of grains of matter in the undeformed positions A and B and deformed positions C and D . This material has suffered a uniform translation and a rigid body rotation.

The strain e_{ij} is evaluated at the unstressed position of the material. As mentioned in Section 11.2.1, however, we commit a negligible error by evaluating it at the stressed position of the material.

The strain has been defined in such a way that it has the transformation properties of a tensor. This purely mathematical fact is shown in the next section.

11.2.1b The Strain as a Tensor

We can confirm that the components e_{ij} form a tensor by using the fact that the displacement δ is a vector. Our discussion here parallels that given in Section 8.2.2 in which we used the transformation properties of the vector traction τ to show that the stress was a tensor. In a similar way we begin here with the transformation of δ to a primed coordinate system:

$$\delta'_i = a_{il}\delta_l. \tag{11.2.17}$$

A discussion of this vector transformation and the direction cosines a_{il} was given in Section 8.2.2 and is summarized in Appendix G.

It follows from (11.2.17) that since components of a_{il} are not functions of x_i

$$\frac{\partial \delta'_i}{\partial x'_j} = a_{il} \frac{\partial \delta_l}{\partial x'_j} = a_{il} \frac{\partial x_k}{\partial x'_j} \frac{\partial \delta_l}{\partial x_k}. \tag{11.2.18}$$

The position vector $\mathbf{r} = x_1\mathbf{i}_1 + x_2\mathbf{i}_2 + x_3\mathbf{i}_3$ is also transformed from a primed coordinate system by an equation in the form of [see (8.2.18) and (8.2.19)]

$$x_k = a_{jk}x'_j; \tag{11.2.19}$$

from this expression it follows that

$$\frac{\partial x_k}{\partial x'_j} = a_{jk} \quad (11.2.20)$$

and (11.2.18) becomes

$$\frac{\partial \delta'_i}{\partial x'_j} = a_{il} a_{jk} \frac{\partial \delta_l}{\partial x_k}. \quad (11.2.21)$$

The steps leading to this equation can be repeated with the indices i and j reversed.

The strain e'_{ij} in the primed coordinate system is by definition

$$e'_{ij} = \frac{1}{2} \left(\frac{\partial \delta'_i}{\partial x'_j} + \frac{\partial \delta'_j}{\partial x'_i} \right). \quad (11.2.22)$$

The first derivative on the right in this expression is replaced by (11.2.21), whereas the second derivative is replaced by (11.2.21), with i and j reversed:

$$e'_{ij} = \frac{1}{2} \left(a_{il} a_{jk} \frac{\partial \delta_l}{\partial x_k} + a_{jl} a_{ik} \frac{\partial \delta_l}{\partial x_k} \right). \quad (11.2.23)$$

We are required to sum over the indices l and k , and so these indices can be reversed in the second term on the right-hand side of this expression, which then becomes the desired transformation equation for e_{ij} :

$$e'_{ij} = a_{ik} a_{jl} e_{kl}. \quad (11.2.24)$$

This expression for the transformation of the strain is the same as that found in Section 8.2.2 for the transformation of the stress T_{ij} ; for example, the expressions for the components of stress in a cylindrical coordinate system, as derived in Example 8.2.5, could also be used here by replacing $T_{ij} \rightarrow e_{ij}$.

11.2.2 Stress-Strain Relations

Our objective in defining the strain was to provide a function of the material displacements δ that could be directly related to the stress. The relations between the components of strain and stress depend on material properties. A particular stress-strain relation was discussed in Section 9.1, in which the modulus of elasticity was introduced as an experimentally determined constant of proportionality between a one-dimensional normal stress and strain*. In this section we generalize this simple stress-strain relation to three-dimensional isotropic solids but again confine ourselves to those solids that can be modeled by an algebraically linear dependence of strain on the stress. This is not unduly restrictive because virtually all elastic media of interest to us are represented adequately by this model. In any case the stress-strain relations are ultimately empirical. Therefore it is reasonable to propose several simple experiments that lead to an understanding of them.

* See Table 9.2, Appendix G.

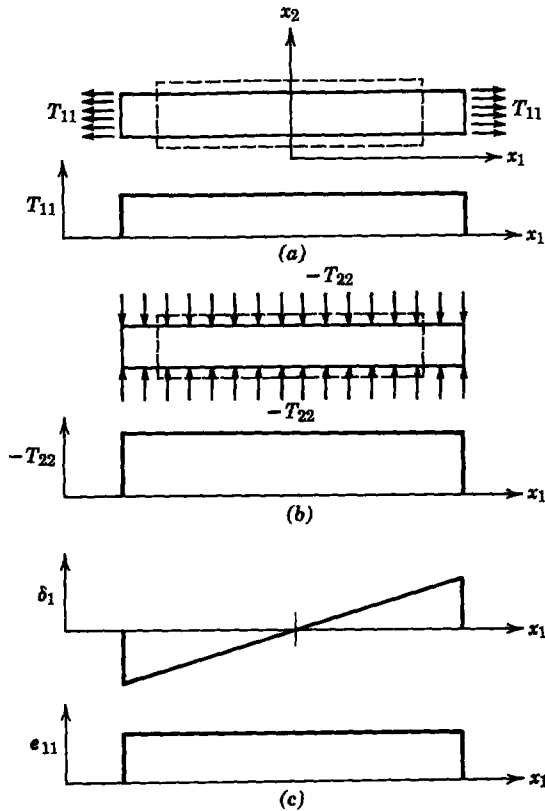


Fig. 11.2.5 (a) Deformations of a block due to a uniform normal stress T_{11} ; (b) deformations identical to (a) produced by a uniform normal stress $-T_{22}$; (c) displacement and normal strain in the x_1 -direction for both (a) and (b).

First, the effect of applying a normal stress to a block of material is considered. In Fig. 11.2.5 two ways of applying a normal stress are shown. Both can result in the same deformation of the material. A normal stress T_{11} is applied to the x_1 -surfaces of the block in Fig. 11.2.5a; the result is elongation of the block in the x_1 -direction. If no stresses are applied to the x_2 (or x_3)-surfaces, there is, in addition, a contraction of the material in the x_2 (and x_3)-directions. This “necking down” of the material is familiar to anyone who has observed what happens when a rubber band is stretched.

Figure 11.2.5b shows the same deformation of the bar as in Fig. 11.2.5a, except that the stress is now compressional and normal to the x_2 -surfaces. Here the material is “squeezed out” in the x_1 -directions by the stress T_{22} , which also reduces the thickness of the block. The x_1 -displacement $\delta_1(x_1)$ of the block in each situation is shown in Fig. 11.2.5c. We see that e_{11} is

uniform over the length of the bar. In Fig. 11.2.5 the block is assumed to be constrained so that there are no displacements in the x_3 -direction. Of course, in three-dimensional displacements a stress T_{11} could also produce displacements in the x_3 -direction and a stress T_{33} could produce displacements in the x_1 -direction.

To account for this experiment two constants E and ν are defined such that

$$e_{11} = \frac{1}{E} [T_{11} - \nu(T_{22} + T_{33})]. \quad (11.2.25)$$

This equation provides that a negative T_{22} can produce the same strain e_{11} as a positive T_{11} . The x_3 -direction is equivalent to the x_2 -direction in our experiment, hence T_{33} enters in (11.2.25) in the same way as T_{22} .

Because the material is isotropic, we can make the same arguments for the other components of the strain and write

$$e_{22} = \frac{1}{E} [T_{22} - \nu(T_{33} + T_{11})], \quad (11.2.26)$$

$$e_{33} = \frac{1}{E} [T_{33} - \nu(T_{11} + T_{22})]. \quad (11.2.27)$$

As pointed out in Chapter 9, E is called the modulus of elasticity, or Young's modulus, and (11.2.25) reduces to the stress-strain relation for a thin rod by setting $T_{22} = T_{33} = 0$. We comment further on the significance of this approximation in Section 11.4. The constant ν , which accounts for the necking down of the material in Fig. 11.2.5a, is called *Poisson's ratio*. Materials that are isotropic, hence could possibly be modeled by (11.2.25) to (11.2.27), are usually a conglomeration of minute crystals. Although each individual crystal is not isotropic, the conglomeration is isotropic on a macroscale. The physical properties of such materials are extremely difficult to predict. For this reason E and ν may be regarded as experimentally determined constants.

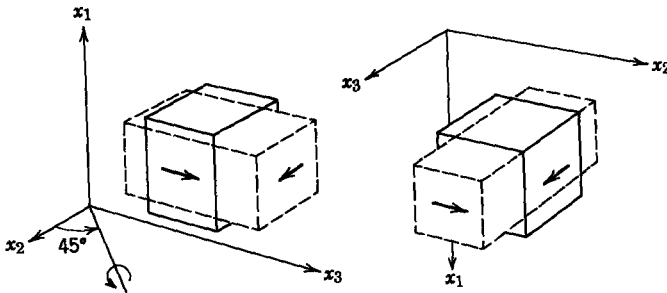


Fig. 11.2.6 Hypothetical situation in which a normal strain results from a shear stress.

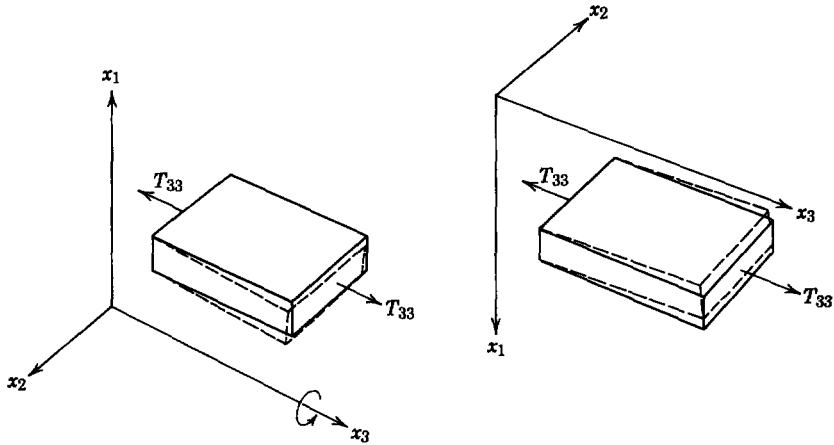


Fig. 11.2.7 Hypothetical situation in which a shear strain results from a normal stress.

In writing (11.2.25) to (11.2.27), we have not only assumed that the material is isotropic but that the normal strains do not depend on the shear stresses. A simple mental experiment shows that these assumptions are the same. Suppose a situation occurs in which normal strain results from a shear stress, as shown in Fig. 11.2.6. A rotation of the coordinates makes it evident that the same stress would give a very different strain, a result that contradicts our assumption of an isotropic material (a material with properties that do not depend on the orientation of the coordinates relative to the material).

This same kind of isotropy argument can be used to show that shear strains cannot depend on normal stresses. Now the conjecture is that we have shear strains that result from normal stresses, as shown in Fig. 11.2.7. Again, a rotation of the coordinate system as shown requires that the same normal stress produce the opposite shear strain.

Physical intuition tells us that each shear strain should be proportional to the corresponding shear stress. As an example, Fig. 11.2.8 shows a block of material subject to the shear stresses T_{13} and T_{31} . The change in angle

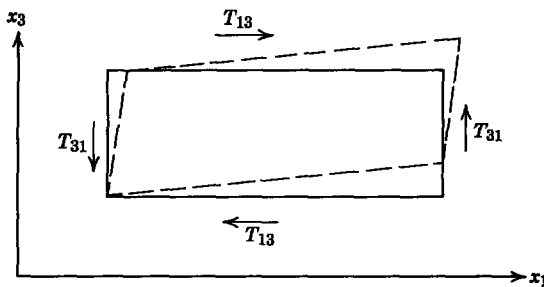


Fig. 11.2.8 The shear strain e_{13} results from the shear stresses T_{13} and T_{31} .

between the originally perpendicular sides of the block is in direct proportion to the applied stress. Hence

$$e_{ij} = \frac{T_{ij}}{2G}, \quad i \neq j, \tag{11.2.28}$$

where G is an experimentally determined constant called the *shear modulus*. In drawing Fig. 11.2.8 we have assumed that $T_{13} = T_{31}$, for otherwise there would be a net torque on the material. This assumption is implicit in (11.2.8), for we have already shown that $e_{ij} = e_{ji}$ (11.2.10).

Given the stress, we can use (11.2.25) to (11.2.28) to find any component of the strain. If, however, we made independent measurements of ν , E , and G , we would be expending more effort than necessary, since, in fact, these constants are related. An example illustrates this point.

Example 11.2.1. Figure 11.2.9 shows a cube of material that is subject to the shear stresses $T_{12} = T_{21} = T_0$ in the x_1, x_2, x_3 -coordinate system. It is clear from this diagram that the components of the stress, viewed from the x'_1, x'_2, x'_3 -coordinate system, are not in

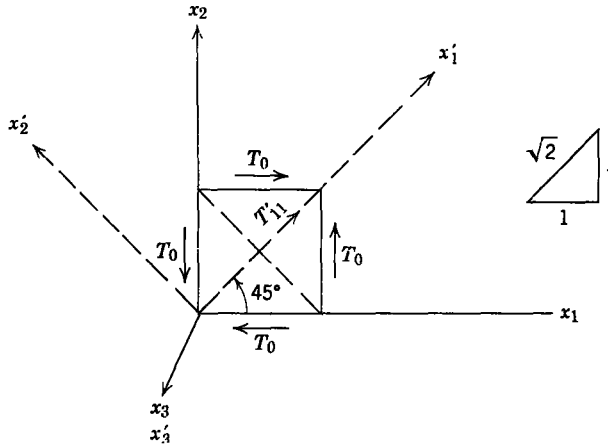


Fig. 11.2.9 A simple example of a pure shear in the x_j frame which transforms into a pure tension and compression in the x'_i frame.

shear but in tension and compression. It is because of this fact that E , ν , and G are not independent constants. A calculation of the strain e'_{ij} , viewed in the x'_i -frame serves to illustrate this point.

The x'_i -coordinates of a point in space can be found from the x_j -coordinates by the transformation $x_i = a_{ij}x_j$ (Section 8.2.2 or Appendix G), in which

$$a_{ij} = \begin{bmatrix} \frac{1}{\sqrt{2}} & \frac{1}{\sqrt{2}} & 0 \\ -\frac{1}{\sqrt{2}} & \frac{1}{\sqrt{2}} & 0 \\ 0 & 0 & 1 \end{bmatrix}. \tag{a}$$

We are given that the material supports the stress

$$T_{ij} = \begin{bmatrix} 0 & T_0 & 0 \\ T_0 & 0 & 0 \\ 0 & 0 & 0 \end{bmatrix}, \quad (b)$$

hence from (11.2.28) that the material undergoes the strain

$$e_{ij} = \begin{bmatrix} 0 & \frac{T_0}{2G} & 0 \\ \frac{T_0}{2G} & 0 & 0 \\ 0 & 0 & 0 \end{bmatrix}. \quad (c)$$

The advantage of writing the stress and strain as tensors is that their components can be found in the x'_i -frame by means of the transformations $T'_{ij} = a_{ik}a_{jl}T_{kl}$ and $e'_{ij} = a_{ik}a_{jl}e_{kl}$. Hence from the last three equations it follows that

$$e'_{ij} = \begin{bmatrix} \frac{T_0}{2G} & 0 & 0 \\ 0 & -\frac{T_0}{2G} & 0 \\ 0 & 0 & 0 \end{bmatrix} \quad (d)$$

and

$$T'_{ij} = \begin{bmatrix} T_0 & 0 & 0 \\ 0 & -T_0 & 0 \\ 0 & 0 & 0 \end{bmatrix}, \quad (e)$$

or, as we suspected, the components of the stress and strain are purely diagonal. Because the material is isotropic, the stress-strain relations must hold, regardless of the coordinate system; that is, (11.2.25) to (11.2.28) must also hold for e'_{ij} and T'_{ij} , and it follows from the above equations that

$$\frac{T_0}{2G} = \frac{1}{E}(T_0 + \nu T_0) \quad (f)$$

or

$$G = \frac{E}{2(1 + \nu)}. \quad (g)$$

This result is important, for it indicates that there are only two independent constants necessary to define the stress-strain relations for an isotropic material; for example, given the modulus of elasticity E and Poisson's ratio ν , the shear modulus G can be found from (g).

Characteristic values of ν and G are given in Table 11.2.1.

Table 11.2.1 Shear Modulus and Poisson's Ratio for Various Materials*

Material	G -units of 10^{10} N/m ²	ν
Aluminum (pure and alloy)	2.55–3.65	0.32–0.34
Brass (60–70% Cu, 40–30% Zn)	3.6–4.1	0.33–0.36
Copper	4.0–4.6	0.33–0.36
Iron, cast (2.7–3.6% C)	3.6–5.6	0.21–0.30
Steel (carbon and low alloy)	7.6–8.2	0.26–0.29
Stainless steel (18% Cr, 8% Ni)	7.3	0.30
Titanium (pure and alloy)	4.1	0.34
Glass	2.6–3.2	0.21–0.27

* See Table 9.1 Appendix G for references and values of E , ρ , and $\sqrt{E/\rho}$.

11.2.3 Summary of Equations

We shall be occupied with electromechanical problems in which the stress T_{ij} and the displacement δ_i are the important variables. Therefore it is desirable to eliminate the strain as a variable from (11.2.25) through (11.2.28).

For the off-diagonal terms this leads directly to the stress as a function of the displacement, but for the diagonal terms three simultaneous conditions on the components T_{11} , T_{22} , and T_{33} result:

$$\begin{aligned}
 e_{11} &= \frac{1}{E} [T_{11} - \nu(T_{22} + T_{33})] = \frac{\partial \delta_1}{\partial x_1}, \\
 e_{22} &= \frac{1}{E} [T_{22} - \nu(T_{33} + T_{11})] = \frac{\partial \delta_2}{\partial x_2}, \\
 e_{33} &= \frac{1}{E} [T_{33} - \nu(T_{11} + T_{22})] = \frac{\partial \delta_3}{\partial x_3}.
 \end{aligned} \tag{11.2.29}$$

These equations can be solved for T_{11} , T_{22} , and T_{33} in terms of the derivatives of δ to provide the diagonal terms in the expression (remember, we sum on a subscript that appears twice),

$$T_{ij} = \begin{bmatrix} 2G \frac{\partial \delta_1}{\partial x_1} + \lambda \frac{\partial \delta_k}{\partial x_k} & G \left(\frac{\partial \delta_1}{\partial x_2} + \frac{\partial \delta_2}{\partial x_1} \right) & G \left(\frac{\partial \delta_1}{\partial x_3} + \frac{\partial \delta_3}{\partial x_1} \right) \\ G \left(\frac{\partial \delta_2}{\partial x_1} + \frac{\partial \delta_1}{\partial x_2} \right) & 2G \frac{\partial \delta_2}{\partial x_2} + \lambda \frac{\partial \delta_k}{\partial x_k} & G \left(\frac{\partial \delta_2}{\partial x_3} + \frac{\partial \delta_3}{\partial x_2} \right) \\ G \left(\frac{\partial \delta_3}{\partial x_1} + \frac{\partial \delta_1}{\partial x_3} \right) & G \left(\frac{\partial \delta_3}{\partial x_2} + \frac{\partial \delta_2}{\partial x_3} \right) & 2G \frac{\partial \delta_3}{\partial x_3} + \lambda \frac{\partial \delta_k}{\partial x_k} \end{bmatrix}, \tag{11.2.30}$$

where (g) of Example 11.2.1 has been used to reduce the number of constants to two and λ is an elastic constant given by

$$\lambda = \frac{\nu E}{(1 + \nu)(1 - 2\nu)}. \quad (11.2.31)$$

The off-diagonal terms in 11.2.30 are given by (11.2.28). The parameter λ has been introduced purely for convenience and is sometimes called the Lamé constant.

The expression for the stress in terms of the displacements, given by (11.2.30), can be summarized in a compact form by using the Kronecker delta function introduced in Section 8.1.

$$T_{ij} = G \left(\frac{\partial \delta_i}{\partial x_j} + \frac{\partial \delta_j}{\partial x_i} \right) + \lambda \delta_{ij} \frac{\partial \delta_k}{\partial x_k}. \quad (11.2.32)$$

Remember that $\delta_{ij} = 0$ for $i \neq j$ [the off-diagonal terms in (11.2.30)], whereas $\delta_{ij} = 1$ if $i = j$ [the diagonal terms in (11.2.30)].

If there are no other forces acting on the elastic material besides the force arising from the elastic stresses given by (11.2.32), we shall have completed the task of finding the equations of motion for the material; that is, the stress given by (11.2.32) can be substituted into the force equation (11.1.4) to provide one vector equation for δ . In this equation the force density of elastic origin is $F_i = \partial T_{ij} / \partial x_j$. It is often more convenient to write the force density in vector notation. The following manipulations illustrate the use of tensor notation.

First, we simply write out the tensor divergence of (11.2.32):

$$F_i = \frac{\partial T_{ij}}{\partial x_j} = G \left(\frac{\partial^2 \delta_i}{\partial x_j \partial x_j} + \frac{\partial^2 \delta_j}{\partial x_i \partial x_j} \right) + \lambda \delta_{ij} \frac{\partial^2 \delta_k}{\partial x_j \partial x_k}. \quad (11.2.33)$$

The first term on the right will be recognized as $G \nabla^2 \delta$, the second is the i th component of $G \nabla(\nabla \cdot \delta)$ and the last has value only when $i = j$ so that it is the i th component of $\lambda \nabla(\nabla \cdot \delta)$. Hence we can write (in vector notation)

$$\mathbf{F} = G \nabla^2 \delta + (G + \lambda) \nabla(\nabla \cdot \delta). \quad (11.2.34)$$

It must be remembered that $\nabla^2 \delta$ is a vector Laplacian defined by $\nabla^2 \delta = \nabla(\nabla \cdot \delta) - \nabla \times (\nabla \times \delta)$, so that (11.2.34) can also be written

$$\mathbf{F} = (2G + \lambda) \nabla(\nabla \cdot \delta) - G \nabla \times (\nabla \times \delta). \quad (11.2.35)$$

This is a useful form of the force density because the material displacements leading to $\nabla \cdot \delta$ and $\nabla \times \delta$ are easily visualized. We defer this point until Section 11.4.

The elastic forces, represented by (11.2.35), are held in dynamical equilibrium by other forces that act on the material. As pointed out in Section 11.1,

Table 11.2.2 Equations Which Describe the Motions of Isotropic Perfectly Elastic Media

Force equation

$$\rho \frac{\partial^2 \delta_i}{\partial t^2} = \frac{\partial T_{ij}}{\partial x_j} + (F_{ex})_i \quad (\text{tensor form}) \quad (11.1.4)$$

$$\rho \frac{\partial^2 \delta}{\partial t^2} = (2G + \lambda) \nabla(\nabla \cdot \delta) - G \nabla \times (\nabla \times \delta) + F_{ex} \quad (\text{vector form}) \quad (11.2.35)$$

Stress equation

$$T_{ij} = 2G e_{ij} + \lambda \delta_{ij} e_{kk} \quad (\text{Hooke's law}) \quad (11.2.32)$$

$$T_{ij} = G \left(\frac{\partial \delta_i}{\partial x_j} + \frac{\partial \delta_j}{\partial x_i} \right) + \lambda \delta_{ij} \frac{\partial \delta_k}{\partial x_k} \quad (\text{stress-displacement}) \quad (11.2.32)$$

Strain equation

$$e_{ij} = \frac{1}{2} \left(\frac{\partial \delta_i}{\partial x_j} + \frac{\partial \delta_j}{\partial x_i} \right) \quad (\text{strain-displacement}) \quad (11.2.10)$$

$$e_{ij} = \frac{1}{2G} T_{ij} - \frac{\nu}{E} \delta_{ij} T_{kk} \quad (\text{Hooke's law}) \quad (11.2.28)$$

$$(11.2.29)$$

Relations among constants

$$\lambda = \frac{\nu E}{(1 + \nu)(1 - 2\nu)} \quad (11.2.31)$$

$$G = \frac{E}{2(1 + \nu)} \quad (\text{g) of Example 11.2.1}$$

one of these forces (per unit volume) is an inertial force. In addition, there may be force densities produced by gravity or electromagnetic fields. The last two externally produced forces are called F_{ex} in the summary of equations given in Table 11.2.2. Other basic equations and relations of elasticity are shown in Table 11.2.2; equation numbers indicate their places in the text.

11.3 ELECTROMECHANICAL BOUNDARY CONDITIONS

Electromechanical coupling with elastic media often occurs through boundary conditions. One-dimensional illustrations of this type of problem were given in Sections 9.1.2. and 9.2.2, in which the boundary condition entered as the requirement of equilibrium for a mechanical terminal pair. In these examples the boundary condition related the stress and displacement at a given point in space. In this section we consider the more general three-dimensional situation.

Boundary conditions are required to describe solutions for the stress and displacement in a region in which material properties undergo abrupt changes. We have made general comments about boundary conditions in connection with the magnetic and electric field equations (Section 6.2)*. We have assumed that the field equations hold in the region of the discontinuity and performed integrations of these equations over the appropriate volumes or surfaces to provide the required "jump" conditions on the fields. Although the displacement vector and stress, like the electric and magnetic fields, are defined by differential equations that can be integrated through an abrupt change in material properties, the analogy is not complete. We were able to assume that Maxwell's equations applied throughout all the volume of interest. The equations of elasticity, however, apply only to a region occupied by an elastic solid and not, for example, to an adjoining region filled with fluid. Hence the boundary conditions resulting from an integration of (11.2.35) over a volume enclosing a section of the interface between two elastic materials are restricted to problems involving just elastic materials. Actually, the situation is not so complicated because a variety of physical problems is modeled by equations in the *form* of (11.1.4), if we are willing to recognize the stress T_{mn} as the total stress acting on the material. Because in writing this equation there are no implications regarding the relationship between T_{mn} and the material motions, we can use (11.1.4) to write a boundary condition of some generality.

In Section 11.1 it was pointed out that because the displacements δ are small no distinction need be made between the Lagrangian and Eulerian representations. We find it convenient here to view the equations of motion as though they were written in Lagrangian coordinates, that is, as though (x_1, x_2, x_3) denoted the unstrained position of the particle that is instantaneously displaced from (x_1, x_2, x_3) by the amount $\delta(x_1, x_2, x_3)$. We can define a surface in three dimensions by the equations

$$\begin{aligned}x_1 &= a(u, v), \\x_2 &= b(u, v), \\x_3 &= c(u, v),\end{aligned}\tag{11.3.1}$$

where (u, v) are parameters, each pair of which defines a particular point on the boundary. When the boundary deforms, due to a material strain, particles on the boundary are then found at the position

$$\begin{aligned}x_1 &= a + \delta_1(a, b, c, t), \\x_2 &= b + \delta_2(a, b, c, t), \\x_3 &= c + \delta_3(a, b, c, t).\end{aligned}\tag{11.3.2}$$

Hence the motion of a particular particle on the boundary in the unstrained position (a, b, c) is defined by (11.3.2). We now consider the situation in

* See Table 6.1, Appendix G.

which elastic media [regions (1) and (2) in Fig. 11.3.1] are joined along the boundary defined by (11.3.2). It is clear that if the boundary is to be well defined one of our boundary conditions is

$$\delta^{(2)}(a, b, c, t) = \delta^{(1)}(a, b, c, t). \tag{11.3.3}$$

This condition can also be considered a necessary consequence of our equations of motion, for if the displacement is not a continuous function the strain, hence the stress (which depends on rates of change of the displacement with respect to position), becomes singular at the boundary.

We are now in a position to integrate (11.1.4) over a small volume that includes the boundary.

$$\int_V \rho \frac{\partial^2 \delta_i}{\partial t^2} dV = \int_V \frac{\partial T_{ij}}{\partial x_j} dV. \tag{11.3.4}$$

The volume V is fixed with its center at the position (a, b, c) , as shown in Fig. 11.3.1. The integration is carried out over the Lagrangian variables (x_1, x_2, x_3) . Hence the time derivative and space integration on the left side of (11.3.4) can be reversed in order. The integral of the divergence of a stress tensor over a volume (see Section 8.1 or Appendix G) can be converted to a surface integral, and (11.3.4) becomes [variations in ρ with time are of the same order as δ , hence are second order in (11.3.4)]

$$\frac{\partial^2}{\partial t^2} \int_V \rho \delta_i dV = \oint_S T_{ij} n_j da. \tag{11.3.5}$$

We consider the situation in which the dimensions of the surfaces A (shown in Fig. 11.3.1) are small compared with the radius of curvature of the boundary but large compared with the thickness Δ of the volume element

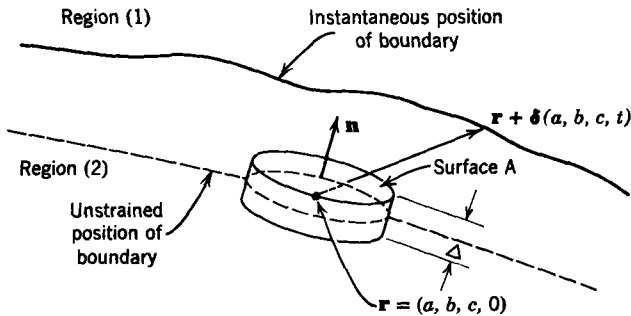


Fig. 11.3.1 Unstrained and strained (instantaneous) interface between regions (1) and (2). A small volume V , with normal \mathbf{n} , encloses a section of the interface. Note that an integration over the volume centered at $(a, b, c, 0)$ is an integration over a volume that remains centered on the moving interface.

Then, if ρ and δ are finite, the volume integral of (11.3.5) vanishes as $\Delta \rightarrow 0$. Sometimes physical situations can be described by an elastic medium, bounded by a heavy layer of material. In these cases the effect of the layer of material is approximated by including a surface mass density ρ_s . Mathematically, the surface mass density is a singularity in the mass density ρ in the same way that the surface charge density is a singularity in the charge density (Section 6.2.2). Then the integral over the volume retains a finite value, and as $\Delta \rightarrow 0$ (11.3.5) can be approximated as

$$\rho_s \frac{\partial^2 \delta_i}{\partial t^2} = [T_{ij}^{(1)} - T_{ij}^{(2)}] n_j, \quad \text{on the boundary,} \quad (11.3.6)$$

where we have divided through by the area A and assumed that the stresses are always finite.

The boundary condition used in Section 9.1.2 was a special case of (11.3.6), in which the stresses T_{ij} were in part due to the elastic strains and in part to a force of electric origin. The condition of (11.3.5) is the continuum-mechanical extension of the requirement used in Chapter 2 that the sum of all forces applied to a mechanical node must be equal to the inertial force associated with that node. The right-hand side of (11.3.6) is the net traction (force per unit area), whereas the left side is an inertial force per unit area.

11.4 WAVES IN ISOTROPIC ELASTIC MEDIA

This section is devoted to establishing a picture of the kinds of dynamical behavior that can be expected in dealing with elastic materials. To this end, we extend the notions introduced in Chapter 9 and recognize that the vibrations of continuous media in three dimensions can also be understood in terms of waves and normal modes. We have already used simple elastic models in Chapters 9 and 10 to illustrate transverse and longitudinal motions in one and two dimensions (the thin rod and membrane). We now consider these motions in three dimensions.

11.4.1 Waves in Infinite Media

In the absence of externally applied forces \mathbf{F}_{ex} the motions of an elastic material are described by (11.2.35), written as

$$\rho \frac{\partial^2 \delta}{\partial t^2} = (2G + \lambda) \nabla(\nabla \cdot \delta) - G \nabla \times (\nabla \times \delta) \quad (11.4.1)$$

This equation is in a particularly convenient form because it makes it possible to distinguish between two essentially different kinds of material displacement. If we take the divergence of (11.4.1), the time and space derivatives can

be permuted to obtain

$$\rho \frac{\partial^2 \psi}{\partial t^2} = (2G + \lambda) \nabla^2 \psi, \quad (11.4.2)$$

where

$$\psi = \nabla \cdot \delta$$

and where use has been made of the identity $\nabla \cdot (\nabla \times \mathbf{A}) \equiv 0$. In the same way the curl of (11.4.1) gives*

$$\rho \frac{\partial^2 \mathbf{C}}{\partial t^2} = G \nabla^2 \mathbf{C}, \quad (11.4.3)$$

where $\mathbf{C} = \nabla \times \delta$ and use has been made of the identity $\nabla \times (\nabla f) \equiv 0$. The scalar function ψ and vector function \mathbf{C} represent kinds of displacement that are analogous to the field intensities \mathbf{E} and \mathbf{H} used to formulate Maxwell's equations. The function ψ can be thought of as a source of the displacement δ in the same sense as the charge density ρ_f is a source of the electric displacement \mathbf{D} [see (1.1.12)]†. Hence the displacements represented by ψ have the same character as the electric displacement that originates or terminates on the charge ρ_f . An intuitive example is shown in Fig. 11.4.1. In a region in which ψ is found to be positive the material displacements tend to diverge. Similarly, the material converges toward regions in which ψ is negative (just as electric lines of force end on negative charge).

Deformations that can be represented by the function ψ are referred to as dilatational, for they represent outward or inward displacements of the material that lead to a change in the volume occupied by the material.

In a similar way \mathbf{C} can be thought of as a "current" that gives rise to a displacement δ in the same way as an electrical current gives rise to a magnetic field \mathbf{H} [see (Eq. 1.1.1)]†. The material displacements tend to follow circular paths about the vector \mathbf{C} , as shown in Fig. 11.4.2.

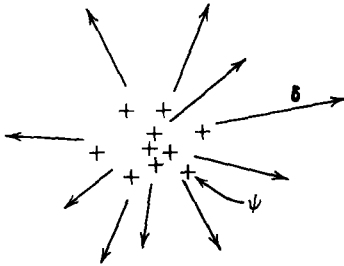


Fig. 11.4.1 Dilatational displacements δ represented by the source function ψ .

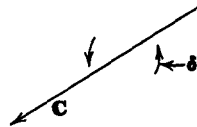


Fig. 11.4.2 Curl displacements represented by \mathbf{C} . The material tends to circulate about the vector field \mathbf{C} .

* $\nabla \times (\nabla \times \mathbf{C}) = \nabla(\nabla \cdot \mathbf{C}) - \nabla^2 \mathbf{C}$

† Table 1.2, Appendix G.

The components of C and the function ψ satisfy equations of the same form. Equations 11.4.2 and 11.4.3 are three-dimensional forms of the wave equation. The essential feature emphasized by these equations [illustrated one-dimensionally by (9.1.13) to (9.1.15)] is the propagating nature of the solutions. Dilatational motions apparently propagate more rapidly than the rotational motions. The wave dynamics are most easily seen by considering two one-dimensional special cases.

Example 11.4.1. Consider a one-dimensional dilatational motion that depends on $x_1 = x$. Then $\partial/\partial x_2 = \partial/\partial x_3 = 0$ and (11.4.2) becomes

$$\frac{\partial^2 \psi}{\partial t^2} = a_c^2 \frac{\partial^2 \psi}{\partial x^2}, \quad (a)$$

where

$$a_c = \left(\frac{2G + \lambda}{\rho} \right)^{1/2}.$$

A discussion of solutions to this wave equation was given in Section 9.1.1. To obtain a physical picture of the mechanics we consider a solution that is sinusoidal in space and time.

$$\psi = \psi_0 \sin \left[\omega \left(t - \frac{x}{a_c} \right) \right]. \quad (b)$$

This solution can be justified by direct substitution into (a) and can be thought of as a wave propagating with the phase velocity a_c in the x -direction.

Within an arbitrary constant that would be determined by the boundary conditions, the actual displacements follow from $\psi = \nabla \cdot \delta$.

$$\delta = \frac{\psi_0 a_c}{\omega} \cos \left[\omega \left(t - \frac{x}{a_c} \right) \right]. \quad (c)$$

At a given instant these displacements appear as shown in Fig. 11.4.3. Note that the material is displaced out of the regions of positive ψ and into regions of negative ψ . We can imagine painting equidistant parallel lines in the unstressed material. Then a wave propagating perpendicular to these lines would distort their relative positions as shown in Fig. 11.4.3b. The material density is increased where the lines are closest together and where ψ is negative. Points of constant phase in the density distribution propagate to the right with the phase velocity a_c . Longitudinal waves of this kind are referred to as *compressional*, *acoustic*, or *dilatational*. Actually, they are a close relative of the compressional waves on a thin rod, encountered in Section 9.1.1. If the expressions for λ and G given in Tables 11.2.2 and 11.4.1 are used to write a_c as a function of E and ν (Poisson's ratio), we obtain

$$a_c = \left(\frac{E}{\rho} \right)^{1/2} N(\nu), \quad (d)$$

where

$$N(\nu) = \left[\frac{1 - \nu}{(1 + \nu)(1 - 2\nu)} \right]^{1/2}.$$

Measured values of ν are given in Table 11.2.1 and can be seen to fall between about 0.2 and 0.5. The function $N(\nu)$ in this range is shown in Fig. 11.4.4 and is greater than 1.

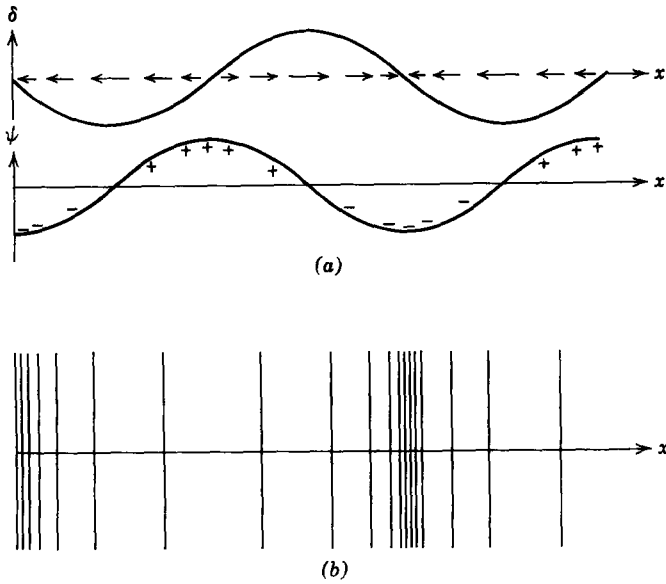


Fig. 11.4.3 Instantaneous view of the displacements δ and source function ψ for a one-dimensional dilatational wave: (a) relative distributions of δ and ψ ; (b) exaggerated appearance of originally equidistant lines painted on the material. Lines compressed together indicate a compression of the material.

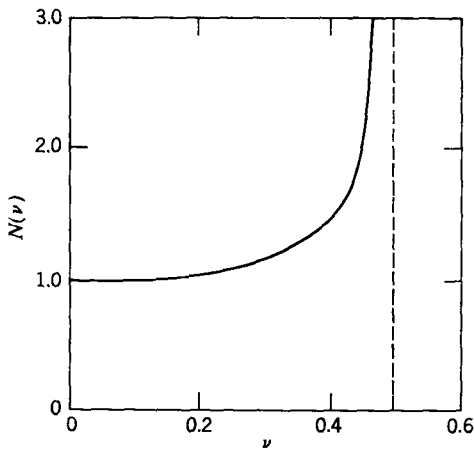


Fig. 11.4.4 The function $N(\nu)$, where ν is Poisson's ratio. Plane dilatational waves propagate with the velocity $a_c = (\sqrt{E/\rho})N$, whereas waves on a thin rod have the velocity $\sqrt{E/\rho}$. Hence N is the ratio of a_c to the acoustic velocity on a thin rod.

Remember that Poisson's ratio entered in the stress-strain relations because a longitudinal stress could lead to transverse displacements (Fig. 11.2.5). By assuming that the material motions were one-dimensional in nature, we have required that there be no transverse displacements. This means that there is a transverse stress (T_{22} or T_{33}) that can be computed from (11.2.26) and (11.2.27) with $e_{22} = e_{33} = 0$; for example,

$$T_{22} = \frac{\nu(1 + \nu)}{1 - \nu^2} T_{11}. \quad (e)$$

This stress tends to constrain the material from the sides and, through Poisson's ratio, to stiffen the material to longitudinal deformations. For this reason we have found a phase velocity a_c that always exceeds the velocity of waves on a thin rod $\sqrt{E/\rho}$. In the thin rod the transverse stresses are zero because of the free surfaces on the rod and longitudinal motions are not affected by Poisson's ratio. We see now that there are actually transverse material displacements on a thin rod. This point is discussed further in Section 11.4.2a, where we define the conditions under which a thin rod model can be used.

Dilatational waves involve normal stresses and normal strains. By contrast the rotational motions constitute a shearing of the medium. The next example illustrates these shear deformations in a one-dimensional case.

Example 11.4.2. In one dimension ($x_1 = x$) the rotational equations (11.4.3) become

$$\frac{\partial^2 C_2}{\partial t^2} = a_s^2 \frac{\partial^2 C_2}{\partial x^2}, \quad (a)$$

$$\frac{\partial^2 C_3}{\partial t^2} = a_s^2 \frac{\partial^2 C_3}{\partial x^2}, \quad (b)$$

where $a_s = \sqrt{G/\rho}$ and because $\partial/\partial x_2 = \partial/\partial x_3 = 0$, $C_1 = 0$. By definition, the components C_2 and C_3 are related to the displacement by

$$C_2 = -\frac{\partial \delta_3}{\partial x}, \quad C_3 = \frac{\partial \delta_2}{\partial x}. \quad (c)$$

Once again, the equations of motion (a) and (b) are wave equations. Now, however, the phase velocity a_s of the waves is less than the compressional wave velocity a_c in Example 11.4.1 and the corresponding material deformations are altogether different. The component C_2 represents displacements in the x_3 -direction. Similarly, C_3 represents transverse motions of the elastic material in the x_2 -direction. Because the stresses and strains are in shear rather than compression, transverse waves of this kind are referred to as *shear waves* or *waves of distortion*.

If we assume that the boundary conditions are such that only C_3 is excited, a traveling wave solution to (b) appears as shown in Fig. 11.4.5. In this figure the material displaces in the x_2 -direction or in a direction that is perpendicular to both C_3 and the direction of propagation. Note that material tends to rotate about the vector C (Fig. 11.4.2) and that the local material density does not change as it did in the dilatational waves.

In this section we have seen that in an infinite medium we can separate rotational or shearing deformations from dilatational motions. Except in a few simple cases, elastic materials deform in such a way that both shearing

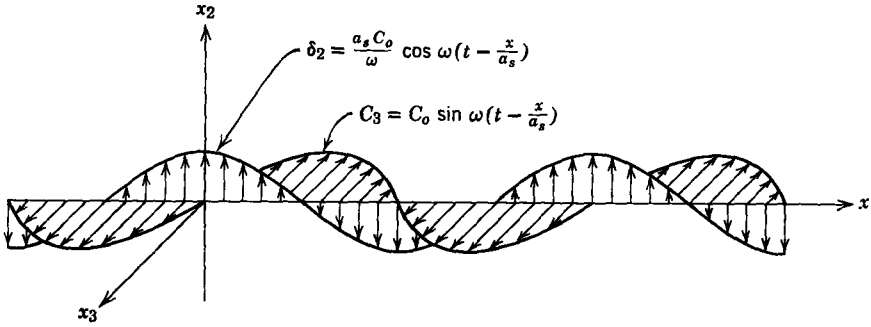


Fig. 11.4.5 Traveling shear wave, showing the spacial relation between material displacements δ_2 and the rotational vector component C_3 . Note that material tends to “rotate” about the vector $C_3 \mathbf{i}_3$, as shown in Fig. 11.4.2.

and dilatation are present. This is true because both types of motion must be present to satisfy boundary conditions.

A simple case in which the one-dimensional dilatational motions predicted by (11.4.2) are an exact solution even in the presence of boundaries is shown in Fig. 11.4.6. Here the transverse boundaries of a bar are constrained by rigid walls that prevent transverse motions but do not inhibit longitudinal motions. Given a driving condition at one end and a boundary condition at the other, the problem can be solved in a manner identical to that used for the thin rod in Section 9.1. If, however, the transverse walls constrain the bar in the x -direction or fail to constrain the transverse displacements, the motions are no longer purely dilatational. Shear strains are required to satisfy the boundary conditions.

The block of material shown in Fig. 11.4.7 is subject to boundary conditions that are satisfied by purely shearing motions. Here one edge is rigidly attached to a wall that prevents both perpendicular motion and slip. The opposite end is driven by a time-varying stress $T_{21} = T_0(t)$. The resulting motions are predicted by (11.4.3) if the boundaries transverse to the x -axis are driven by the same time-varying shear stress $T_{21}(x, t)$ (see Example 11.4.3 for a solution), but if these transverse boundaries are constrained by a rigid wall, or are free

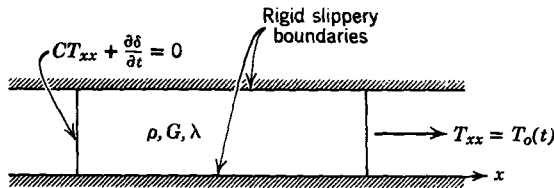


Fig. 11.4.6 An elastic bar with boundaries that permit purely dilatational motions in the x -direction.

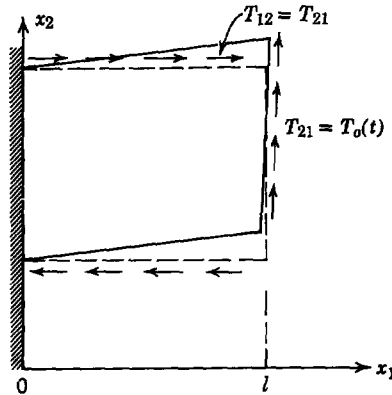


Fig. 11.4.7 An elastic bar with boundaries and driving stresses that permit purely shearing motions in the x_2 -direction.

of stress, the motions must include a dilatational part; that is, any other boundary condition than that shown in Fig. 11.4.7 will couple the rotational and dilatational motions.

Because boundary conditions usually couple the compressional and shearing motions, any dynamical problem will involve a combination of the characteristic velocities a_s and a_c . These velocities are tabulated, along with characteristic values of λ , in Table 11.4.1.

Table 11.4.1 Phase Velocities for Shear and Compressional Waves in an Infinite Medium*

Material	λ (units of 10^{11} N/m ²)	a_s (units of 10^3 m/sec)	a_c (units of 10^3 m/sec)
Aluminum	0.626	3.0	6.35
Brass	1.04	2.2	4.7
Copper	1.17	2.3	4.8
Iron, cast	0.836	2.8	5.2
Steel	1.18	3.2	6.0
Stainless steel	1.19	3.0	5.8
Titanium	0.904	3.0	6.2
Glass	0.366	2.9	5.1

* When ranges of E , ν , and G are given in Tables 9.1 (Appendix G) and 11.2.1, the largest values have been used.

Example 11.4.3. In this example we seek to establish a further familiarity with shearing deformations. Figure 11.4.8 shows a slab of material rigidly attached to a wall at $x = 0$ and driven with a shear stress $T_{21} = \text{Re} [\hat{T}e^{j\omega t}]$ at $x = l$. The slab has infinite extent in the x_2 - and x_3 -directions; hence it is reasonable to assume that the motions are one-dimensional

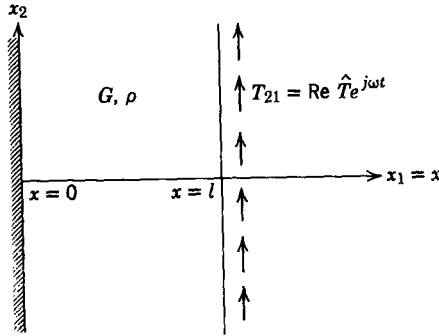


Fig. 11.4.8 An infinite slab of elastic material subjected to the uniformly distributed shear stress $T_{21} = \text{Re}(\hat{T}e^{j\omega t})$ at $x = l$ and fixed at $x = 0$.

($\partial/\partial x_2 = \partial/\partial x_3 = 0$). The following questions are to be answered: (1) What is the displacement of the material as a function of (x, t) ? (2) If boundaries are introduced at $x_2 = 0$ and $x_2 = L$, what boundary conditions are required to make the one-dimensional assumption correct? (3) if the peak shear stress applied at $x = l$ is equal to 1 atm, what is the largest displacement of the material (as an example, consider a slab made of brass, $l = 1$ m, and the low frequency limit at which $\omega \rightarrow 0$). (4) At a frequency of 1 kc what is the least value of l required to produce a resonance?

1. The excitation tends to produce displacements δ_2 , hence we guess that $C_2 = 0$. Our guess is justified if we can satisfy both differential equations and boundary conditions. Equations (b) and (c) of Example 11.4.2 then give

$$\frac{\partial^2 \delta}{\partial t^2} = a_s^2 \frac{\partial^2 \delta}{\partial x^2}, \quad (\text{a})$$

where $\delta_2 = \delta$ and $x_1 = x$. Two boundary conditions are necessary to determine fully the sinusoidal steady-state solution to this equation. These conditions are evident from the statement of the problem

$$T_{21}(l, t) = \text{Re}(\hat{T}e^{j\omega t}) = G \frac{\partial \delta}{\partial x}(l, t) \quad (\text{b})$$

and

$$\delta(0, t) = 0. \quad (\text{c})$$

Now, if we assume solutions with the same frequency as the excitation

$$\delta = \text{Re}(\hat{\delta}e^{j\omega t}), \quad (\text{d})$$

the unknown function $\hat{\delta}(x)$ can be found by substituting (d) into (a) and solving the resulting ordinary differential equation. Hence

$$\hat{\delta} = A \sin kx + B \cos kx, \quad (\text{e})$$

where

$$k = \frac{\omega}{a_s}$$

and A and B are arbitrary constants determined by the boundary conditions. Condition (c) shows that $B = 0$, whereas condition (b) determines A as

$$A = \frac{\hat{T}}{kG \cos kl}. \quad (f)$$

It follows from (d) and (e) that the required solution for the displacement is

$$\delta = \text{Re} \left[\frac{\hat{T} \sin kx e^{j\omega t}}{kG \cos kl} \right]. \quad (g)$$

2. In our solution all displacements are zero except $\delta_2 = \delta$, as given by (g). There are two components of stress (11.2.32). One was used to match the boundary condition at $x = l$:

$$T_{21} = G \frac{\partial \delta}{\partial x} = \text{Re} \left[\frac{\hat{T} \cos kx e^{j\omega t}}{\cos kl} \right]. \quad (h)$$

The other is present because $T_{ij} = T_{ji}$ or, in particular,

$$T_{12} = T_{21}. \quad (i)$$

Hence, if the slab has boundaries at $x_2 = 0$ and $x_2 = L$, our solution will be correct only if there is a shearing stress on these boundaries given by (h) and (i). Note that this stress is a function of both x and t . In the limit at which $L \gg l$, we expect that the stress excitation on the transverse boundaries can be ignored and our one-dimensional solution will be approximately correct, regardless of the boundary conditions at $x_2 = 0$ and $x_2 = L$.

3. In the limit at which $\omega \rightarrow 0$ (quasi-static motions) $k \rightarrow 0$ and (g) shows that the peak δ occurs at $x = l$, where (since $1 \text{ atm} = 1.013 \times 10^5 \text{ N/m}^2$ and G can be found from Table 11.2.1) (g) gives

$$\begin{aligned} |\delta|_{\text{peak}} &= \frac{|\hat{T}|l}{G} = (1.01 \times 10^5)(1)/4.1 \times 10^{10} \\ &= 2.5 \times 10^{-6} \text{ m} \quad \left(\text{about } \frac{1}{10,000} \text{ in.} \right) \end{aligned} \quad (j)$$

We see that static deflections are likely to be very small.

4. The slab is in a resonant state when the denominator of (g) becomes zero or when

$$kl = \frac{n\pi}{2}, \quad n = 1, 3, 5, \dots \quad (k)$$

Hence the smallest value of l that will produce a resonance at 1 kc (a_s in Table 11.4.1) is

$$l = \frac{\pi a_s}{2\omega} = \pi 2.2 \times \frac{10^3}{2(2\pi \times 10^3)} = 0.55 \text{ m}. \quad (l)$$

Under these conditions the 0.55-m thickness of the brass slab represents one quarter of a wavelength.

11.4.2 Principal Modes of Simple Structures

In most dynamical situations involving elastic media boundaries play an important role. Our development makes it natural to think of these boundaries

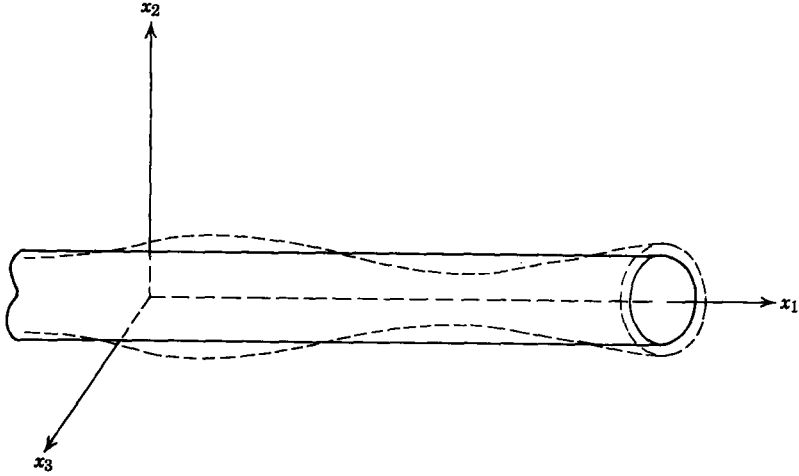


Fig. 11.4.9 A thin elastic rod with a longitudinal axis x_1 and transverse coordinates x_2 and x_3 . An exaggerated transverse distortion of the material is shown as it accompanies longitudinal compression and extension of the rod.

as two types: longitudinal and transverse; that is, the elastic structure usually has one dimension that is greater than the others, such as the x -direction for the thin rod of Fig. 11.4.9, and it is natural to analyze the dynamics in terms of wave propagation in that direction. Conditions applied at discrete positions along the x_1 -axis, referred to as longitudinal boundary conditions, were discussed in Section 9.1.1*b*. The extremities of the material in the x_2 - and x_3 -directions are referred to as transverse boundaries. It is the purpose of this section to introduce the effect that the transverse boundaries have on wave propagation in the longitudinal direction.*

Even in the absence of electromechanical interactions, wave propagation in the presence of material boundaries is an involved subject. It serves our purposes here to consider two cases, both of which make the essential point in a simple way and have practical value. First, we reconsider in the light of three-dimensional elasticity the thin rod. Then in Section 11.4.2*b* the transverse motions of a thin beam are analyzed. In each of these cases it is assumed that the longitudinal wavelengths of interest are large compared with the transverse dimensions. In the general case in which no approximations are made concerning the wavelength, thin elastic structures support an infinite set of modes, each having a different dependence on the transverse coordinates. Most of these modes do not propagate at low frequencies. The waves on a thin rod and on a thin beam, as considered in Sections 11.4.2*a* and 11.4.2*b*,

* For those familiar with the theory of guided electromagnetic waves the waves of Section 11.4.1 are waves in "free space," whereas those discussed here are guided waves analogous to those found in a waveguide.

propagate even as the frequency approaches zero. Among all modes that are generally possible, they assume considerable practical importance and are called the *principal modes* of their respective structures. In Section 11.4.3 we illustrate the nature of the higher order modes by considering the dynamics of a plate subject to a shearing excitation. Here we find that at low frequencies the higher order modes appear as evanescent waves; hence we again encounter the topic of spatially growing (decaying) waves discussed in Section 10.1.2. A detailed presentation of wave propagation in elastic plates and cylinders is of interest* in the design of delay lines and electromechanical filters to be used at high frequencies (e.g., megahertz). At high frequencies the higher order modes are inadvertently excited because longitudinal wavelengths are on the order of the transverse dimensions.

11.4.2a The Thin Rod

A thin elastic rod is shown in Fig. 11.4.9. In static equilibrium it has the geometry of a right circular cylinder, with its axis in the x_1 -direction. An approximate description of the longitudinal motions was given in Section 9.1†. We are interested in having a second look at the dynamics to see what transverse motions of the material are implied by the three-dimensional equations of elasticity. We can argue that the equation of motion is the same as that found in Section 9.1 for longitudinal deformations by observing that the transverse surfaces of the rod are free of externally applied stresses. Hence, if the rod is very thin, the stresses T_{22} , T_{33} (essentially normal to the transverse surface) and T_{12} and T_{13} (essentially the shear stress on the surface) cannot be very different from zero inside the rod. This is the starting point in writing an approximate equation of motion.

Because we take $T_{12} = T_{13} = 0$, the force equation in the x_1 -direction (11.1.4) becomes

$$\rho \frac{\partial^2 \delta_1}{\partial t^2} = \frac{\partial T_{11}}{\partial x_1}. \quad (11.4.4)$$

In addition, because $T_{22} = T_{33} = 0$, (11.2.29) of Table 11.2.2 shows that

$$e_{11} = \frac{\partial \delta_1}{\partial x_1} = \left(\frac{1}{2G} - \frac{\nu}{E} \right) T_{11}, \quad (11.4.5)$$

and because $G = E/2(1 + \nu)$ we obtain

$$T_{11} = E \frac{\partial \delta_1}{\partial x_1}. \quad (11.4.6)$$

* See W. P. Mason, *Physical Acoustics*, Vol. I, Part A, Academic, New York, 1964, p. 111.

† Table 9.2, Appendix G.

This will be recognized as the relation used in Section 9.1. It follows from (11.4.4) and (11.4.6) that the longitudinal displacement is predicted by the equation

$$\rho \frac{\partial^2 \delta_1}{\partial t^2} = E \frac{\partial^2 \delta_1}{\partial x_1^2}. \quad (11.4.7)$$

Although they do not enter in the equation of motion, transverse displacements do accompany $\delta_1(x_1, t)$. They can be computed under the assumption that δ_1 is a known function. From (11.2.32) and the condition that the normal stress on the transverse boundaries be zero we have

$$T_{22} = 0 = (2G + \lambda) \frac{\partial \delta_2}{\partial x_2} + \lambda \left(\frac{\partial \delta_1}{\partial x_1} + \frac{\partial \delta_3}{\partial x_3} \right), \quad (11.4.8)$$

$$T_{33} = 0 = (2G + \lambda) \frac{\partial \delta_3}{\partial x_3} + \lambda \left(\frac{\partial \delta_1}{\partial x_1} + \frac{\partial \delta_2}{\partial x_2} \right). \quad (11.4.9)$$

Presumably, we have solved (11.4.7). Hence these last two equations can be simultaneously solved for $\partial \delta_2 / \partial x_2$ or $\partial \delta_3 / \partial x_3$; for example,

$$\frac{\partial \delta_2}{\partial x_2} = \frac{-\lambda}{2(G + \lambda)} \frac{\partial \delta_1}{\partial x_1}(x_1, t). \quad (11.4.10)$$

The right-hand side of this equation is dependent only on (x_1, t) . Hence it can be integrated to obtain

$$\delta_2 = \frac{-\lambda}{2(G + \lambda)} \frac{\partial \delta_1}{\partial x_1} x_2 + f(x_1, x_3, t), \quad (11.4.11)$$

where f is an arbitrary function determined by the cross-sectional geometry; for example, if the rod is a right-circular cylinder, coaxial with the x_1 -axis, symmetry requires that $\delta_2(x_1, 0, x_3) = 0$ or that $f = 0$. Similarly,

$$\delta_3 = \frac{-\lambda}{2(G + \lambda)} \frac{\partial \delta_1}{\partial x_1} x_3 + g(x_1, x_2, t), \quad (11.4.12)$$

where $g = 0$ for a right-circular cylinder. The last two equations show that the transverse displacements are largest for the material with the greatest distance from the x_1 -axis. In regions in which the rate of change with respect to x_1 is large the transverse displacements are also large.

As an example, consider the traveling wave

$$\delta_1 = \delta_0 \sin(\omega t - kx_1), \quad (11.4.13)$$

where (11.4.7) shows that $\omega = k\sqrt{E/\rho}$. Then from (11.4.11)

$$\delta_2 = \frac{\delta_0 \lambda k x_2}{2(G + \lambda)} \cos(\omega t - kx_1). \quad (11.4.14)$$

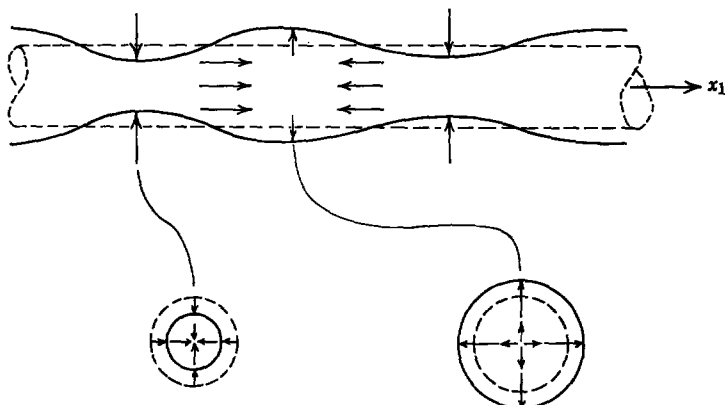


Fig. 11.4.10 An instantaneous view of displacements that accompany a compressional wave traveling in the x_1 -direction on a thin rod. The transverse displacements are exaggerated in this figure.

The displacements represented by the last two equations can be pictured as shown in Fig. 11.4.10.

In retrospect, we see that δ_2 and δ_3 were ignored in the longitudinal force equation and were then found from the predicted displacements δ_1 . This procedure is analogous to a quasi-static analysis (Sections B.2.2 and 9.1.3) in which variations with respect to time are at first ignored and then computed as second-order effects. In the rod, two-dimensional effects are second order and the analysis may be referred to as quasi-one-dimensional. Other quasi-one-dimensional models are introduced in the next section and in Chapter 13. Such models, which reduce the significant effects to a dependence on a single coordinate, are of considerable importance not only in continuum electromechanics but in many other areas as well. Very often they are referred to as “long-wave” limits, because the quasi-one-dimensional model is correct, provided wavelengths in the longitudinal direction are long enough. We can illustrate this point by recognizing that δ_2 is small compared with δ_1 if [from (11.4.13) and (11.4.14)]

$$\frac{\lambda k R}{2(G + \lambda)} \ll 1, \quad (11.4.15)$$

where we have used the rod radius R to evaluate δ_2 . Remember that one wave-length is $2\pi/k$, and we see that (11.4.15) is fulfilled if wavelengths are large compared with the radius R .

11.4.2b The Thin Beam

The principal longitudinal or dilatational mode in the presence of boundaries is the subject of Section 11.4.2a. In this section we consider principal

shearing modes on a thin beam of elastic material. Vibrating reeds or bars (tuning forks), commonly used in electromechanical transducers, provide a familiar context for broadening our understanding of distributed dynamic systems.

By now it is a well-established notion that the dynamics of continuous media are closely related to the propagation of waves. The examples of Chapter 9, which describe thin rods and membranes, illustrate this point. Transverse motions of a beam are similar but involve several complications that prevent a misleading generalization from the simple systems considered so far. We find that beam deflections involve four boundary conditions, compared with the two conditions required for the rods and membranes. As a result, the eigenmodes are not simple sinusoids in space but rather have both propagating and evanescent components and the eigenfrequencies of the beam are not usually harmonics. We have encountered this effect of dispersion before (Chapter 10) but not in so familiar a context. If we clamp the end of a beam (steel ruler) at one end with the other end free, as shown in Fig. 11.4.11, the lowest eigenmode can be excited by releasing the beam from a deflected position. In a rod or membrane halving the length l will double the frequency (which can be measured with a strobrotachometer). As we shall see in Example 11.4.4, the thin beam lacks this property.

Our object is to use the fact that the bar is thin (in the direction of the deflection) to write an equation of motion that contains only the longitudinal coordinate x_1 and the time t . As is usually the case in developing quasi-one-dimensional models, the starting point is motivated physically. A cross-sectional view of the bar, subject to a hypothetical deformation, is shown in Fig. 11.4.12. If there is no equilibrium (static) longitudinal tension on the bar (it is not being stretched in the x_1 -direction as the membrane was*), the displacement of a line painted on the side of the bar will be as shown.

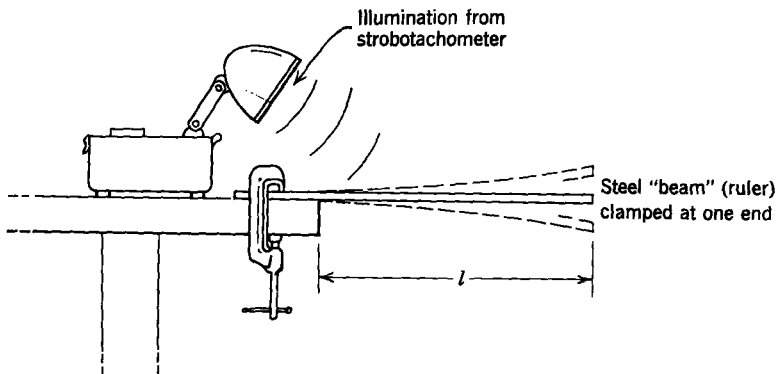


Fig. 11.4.11 The lowest eigenfrequency of a thin beam clamped at one end and free at the other can be measured by using a strobrotachometer.

* See Table 9.2, Appendix G.

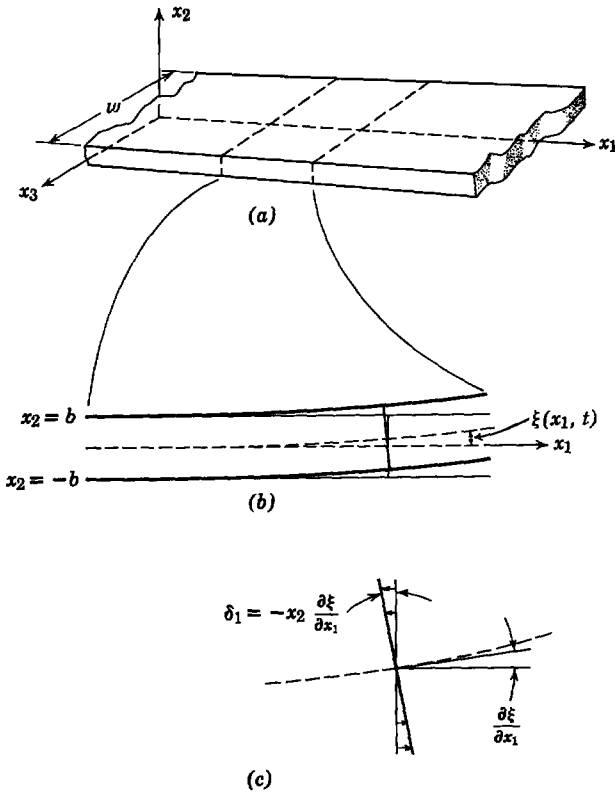


Fig. 11.4.12 Transverse vibrations of a thin bar: (a) in static equilibrium the axis of the bar is in the x_1 -direction with material motions essentially in the x_2 -direction; (b) a small section of the bar shows the deformation of a line perpendicular to the neutral plane; (c) a detailed view of a perpendicular line shows the relation to the transverse displacement ξ of the neutral plane.

Because the bar is not undergoing a net tension, there is an x_2 - x_3 plane (called the neutral plane) in which the material has no x_1 displacement. Then for small deflections of the bar the angle of deflection of a cross-sectional line is given by $\partial \xi / \partial x_1$ (Fig. 11.4.12). The assumption is made that the bar is thin enough that the longitudinal material displacement δ_1 at any cross section can be approximated as having a linear dependence on the transverse dimension x_2 . It follows that this linear dependence is about

$$\delta_1 = -x_2 \frac{\partial \xi}{\partial x_1}(x_1, t). \tag{11.4.16}$$

Then from (11.2.10) the normal strain is

$$e_{11} = \frac{\partial \delta_1}{\partial x_1} = -x_2 \frac{\partial^2 \xi}{\partial x_1^2}(x_1, t). \tag{11.4.17}$$

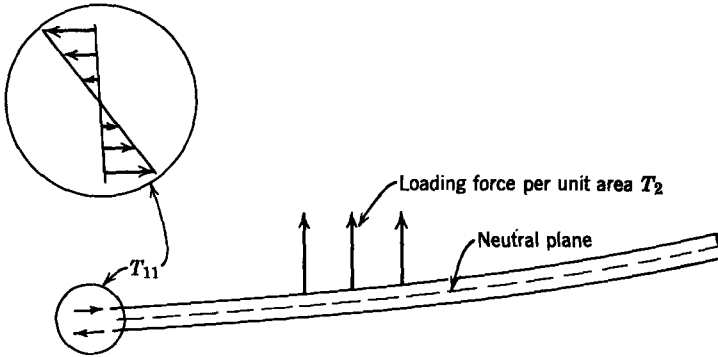


Fig. 11.4.13 Hypothetical beam deflection due to a surface force density T_2 . Because the thickness is small compared with the length, the stresses T_{11} are much greater than either T_{22} or T_{33} .

A second approximation is now made. It is assumed that the strain e_{11} is largely created by T_{11} or that $T_{11} \gg T_{22}$ or T_{33} . A section of the bar is shown in Fig. 11.4.13. Because the bar is thin, the stress T_{22} is on the order of any loading force per unit area T_2 . The stresses T_{11} must hold the vertical forces in force equilibrium, and because the beam is thin compared with its length it is apparent that we must have $T_{11} \gg T_{22}$. Because there are no loading forces in the x_3 -direction, it is even more reasonable that the stresses T_{33} can be ignored, compared with T_{11} . It follows from (11.2.29) that

$$T_{11} = Ee_{11} = -x_2 E \frac{\partial^2 \xi}{\partial x_1^2}. \quad (11.4.18)$$

Altogether, we shall make four approximations based on the thinness of the beam and the transverse nature of the deflections under consideration. The third of these assumptions is now introduced—that the longitudinal inertial force makes no essential contribution to the dynamics. This is reasonable because the deflection considered is mainly in the x_2 -direction. Then the x_1 -component of the momentum equation for the elastic material [see (11.1.4)] becomes

$$\frac{\partial T_{11}}{\partial x_1} = -\frac{\partial T_{12}}{\partial x_2} = -E x_2 \frac{\partial^3 \xi}{\partial x_1^3}. \quad (11.4.19)$$

This expression can be integrated to give

$$T_{12} = \frac{E x_2^2}{2} \frac{\partial^3 \xi}{\partial x_1^3} + g(x_1, t). \quad (11.4.20)$$

The arbitrary function $g(x_1, t)$ is evaluated by requiring that the surfaces at $x_2 = \pm b$ support no shearing stress or that

$$T_{12} = \frac{(x_2^2 - b^2)}{2} E \frac{\partial^3 \xi}{\partial x_1^3}. \quad (11.4.21)$$

The x_2 -component of (11.1.4), the force equation, is

$$\rho \frac{\partial^2 \delta_2}{\partial t^2} = \frac{\partial T_{21}}{\partial x_1} + \frac{\partial T_{22}}{\partial x_2}. \quad (11.4.22)$$

The desired equation of motion can now be found by integrating this equation over an arbitrary cross section of the bar:

$$\rho \frac{\partial^2}{\partial t^2} \int_{-b}^{+b} \delta_2 dx_2 = \int_{-b}^{+b} \frac{\partial T_{21}}{\partial x_1} dx_2 + [T_{22}]_{x_2=b} - [T_{22}]_{x_2=-b}. \quad (11.4.23)$$

As a fourth (and last) approximation, the left-hand side of (11.4.23) is approximated by the product of the cross-sectional thickness $2b$ and the displacement of the bar center. Hence, making use of (11.4.21) and the fact that $T_{12} = T_{21}$,

$$2b\rho \frac{\partial^2 \xi}{\partial t^2} = \frac{\partial^4 \xi}{\partial x_1^4} E \int_{-b}^{+b} \left(\frac{x_2^2 - b^2}{2} \right) dx_2 + T_2, \quad (11.4.24)$$

where T_2 is the sum of the forces per unit area acting on the x_2 -surfaces of the bar and defined by

$$T_2 = [T_{22}]_{x_2=b} - [T_{22}]_{x_2=-b}. \quad (11.4.25)$$

After the integration indicated by (11.4.24) the equation of motion for transverse displacements of the bar becomes

$$\frac{\partial^2 \xi}{\partial t^2} + \frac{Eb^2}{3\rho} \frac{\partial^4 \xi}{\partial x_1^4} = \frac{T_2}{2b\rho}. \quad (11.4.26)$$

The independent variables in this expression are (x_1, t) ; hence we have formulated the dynamics in terms of a quasi-one-dimensional model. Beam deflections can be determined from this last equation, given four boundary conditions which arise because the ends of the beam are clamped in a certain fashion or because the ends are free of shear or normal stresses. To write boundary conditions on δ_1 , T_{11} , and T_{12} in terms of ξ we can use (11.4.16), (11.4.18), and (11.4.21).

The dependence of the longitudinal and shear stresses on the transverse coordinate x_2 is shown in Fig. 11.4.14. Note that the x_2 -dependences of T_{11}

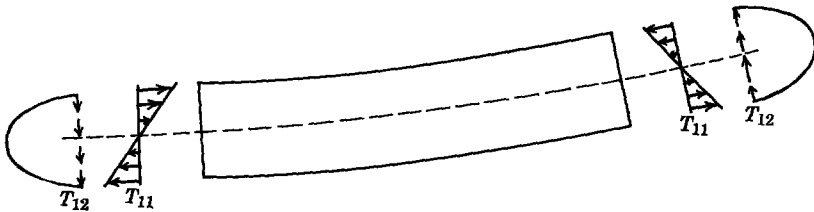


Fig. 11.4.14 Dependence of the normal and shear stresses on the transverse dimension of the beam.

and T_{12} are given by the lowest order polynomial expressions consistent with the requirements that there be no net longitudinal stress and that the shear stresses be zero at the surface of the beam.

Example 11.4.4. The situation shown in Fig. 11.4.15a provides an illustration of the role played by the boundary conditions. A thin beam is clamped at $x = 0$, so that both the transverse and longitudinal displacements of the material at this point are zero. The

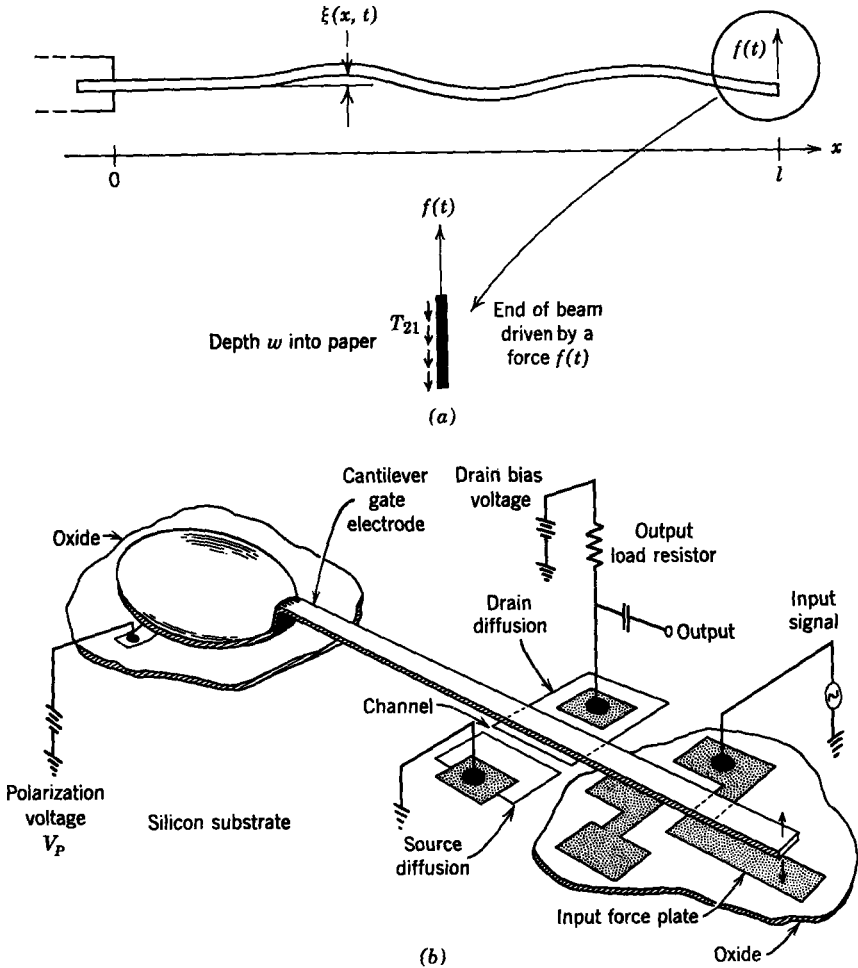


Fig. 11.4.15 (a) A thin elastic beam is driven to vibrate in a direction transverse to its smallest dimension by a force $f(t)$ applied at $x = l$. The end at $x = l$ is free of longitudinal stresses T_{11} , whereas the beam is clamped at $x = 0$. (b) One electromechanical application of the thin elastic beam is illustrated by the “Resonant Gate Transistor” (See W. E. Newell, “Ultrasonics in Integrated Electronics,” *Proc. IEEE*, October 1965) A high Q integrated circuit incorporates an electrostatically driven beam. The elastic beam provides an inherently stable resonant element of extremely small proportions (see Fig. 11.4.15c).

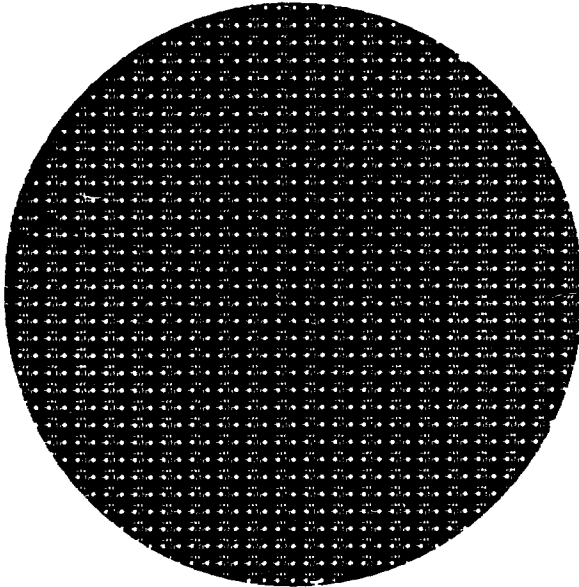


Fig. 11.4.15c Silicon wafer of 1-in. diameter containing nearly 500 resonant gate transistors of the type shown in (b). (Courtesy of Westinghouse Electric Corp.)

opposite end at $x = l$ is free of longitudinal stresses and is set into vibration by a force $f(t)$, which is sinusoidal:

$$f(t) = \text{Re} [\hat{f} e^{j\omega t}]. \quad (\text{a})$$

The sinusoidal steady-state deflections $\xi(x, t)$ are to be found. Of course, to find the driven response, we shall also find the natural frequencies of the beam. In an experiment such as that shown in Fig. 11.4.11 the bar vibrates at these eigenfrequencies. Hence the dependence of the lowest eigenfrequency on the length l will also be found.

The equation of motion is (11.4.26) with $T_2 = 0$. Because the drive assumes a sinusoidal form, we shall guess solutions:

$$\xi = \text{Re} [\hat{\xi}(x) e^{j\omega t}], \quad (\text{b})$$

in which case (11.4.26) requires that

$$\frac{d^4 \hat{\xi}}{dx^4} - \alpha^4 \hat{\xi} = 0, \quad (\text{c})$$

where

$$\alpha = \left[\omega^2 \left(\frac{3\rho}{Eb^2} \right) \right]^{1/4}.$$

The spatial dependence is found from (c) by again guessing exponential solutions $\hat{\xi} = e^{-jkx}$, in which substitution shows that $k^4 = \alpha^4$ or that there are four solutions for the spatial dependence:

$$k = \alpha, -\alpha, j\alpha, \text{ and } -j\alpha. \quad (\text{d})$$

Note that we have defined α as a positive real constant. We have assumed solutions of the form $e^{j(\omega t - kx)}$ and found [from (d)] a pair of waves propagating in each direction on the

beam and a pair of evanescent waves. The evanescent waves are required in addition to the ordinary waves to satisfy the four boundary conditions imposed on the beam. This is in contrast to the situation in Section 10.1.2, in which propagating waves became evanescent at a frequency below some cutoff frequency. Here, all four waves are present simultaneously.

As we have seen, a boundary value problem of this kind is more conveniently solved in terms of trigonometric and hyperbolic functions, rather than complex exponentials (traveling waves). Hence we use linear combinations of the four exponential solutions to write the solution in the form

$$\xi = A \sin \alpha x + B \cos \alpha x + C \sinh \alpha x + D \cosh \alpha x, \quad (e)$$

where A , B , C , and D are to be evaluated by using the boundary conditions.

Because there is no longitudinal or transverse motion of the material at $x = 0$, two boundary conditions are

$$\xi(0) = 0, \quad (f)$$

$$\frac{d\xi}{dx}(0) = 0, \quad (g)$$

where (g) follows from the expression for δ_1 given by (11.4.16). Because $T_{11} = 0$ at $x = l$, (11.4.18) shows that

$$\frac{d^2\xi}{dx^2}(l) = 0. \quad (h)$$

The fourth boundary condition arises from the transverse force equilibrium of the beam at $x = l$. The force $f(t)$ acts on a thin element of the beam at $x = l$, as shown in Fig. 11.4.15a. This force is held in equilibrium by the shear stress T_{21} . Hence, since the volume of material within the element is vanishingly small (there is no singularity of mass at the end of the beam), we can write (note that $T_{12} = T_{21}$)

$$f = w \int_{-b}^b T_{12} dx_2. \quad (i)$$

The boundary condition at $x = l$ in terms of ξ follows by using (11.4.21) to find

$$\hat{f} = \frac{wE}{2} \frac{d^3\xi}{dx^3} \int_{-b}^b (x_2^2 - b^2) dx_2 \quad (j)$$

or

$$\hat{f} = -\frac{2w}{3} Eb^3 \frac{d^3\xi}{dx^3}(l). \quad (k)$$

The first two boundary conditions show that

$$D = -B, \quad (l)$$

$$C = -A. \quad (m)$$

These two relations, together with the second two boundary conditions, give the equations

$$\begin{aligned} A[\sin \alpha l + \sinh \alpha l] + B[\cos \alpha l + \cosh \alpha l] &= 0, \\ A[\cos \alpha l + \cosh \alpha l] - B[\sin \alpha l - \sinh \alpha l] &= 2\hat{F}, \end{aligned} \quad (n)$$

where

$$\hat{F} = \frac{3\hat{f}}{wE4b^3\alpha^3}.$$

Equations (n) provide simultaneous expressions for A and B which are solved to provide

$$A = \frac{\hat{F}(\cos \alpha l + \cosh \alpha l)}{1 + \cosh \alpha l \cos \alpha l}, \tag{o}$$

$$B = \frac{-\hat{F}(\sin \alpha l + \sinh \alpha l)}{1 + \cosh \alpha l \cos \alpha l}. \tag{p}$$

To make this manipulation we have used the identities $\cos^2 x + \sin^2 x = 1$ and $\cosh^2 x - \sinh^2 x = 1$. The constants D and C follow from (l) and (m) to complete the solution for ξ given by (e).

$$\xi = \hat{F} \left[\frac{(\cos \alpha l + \cosh \alpha l)(\sin \alpha x - \sinh \alpha x) - (\sin \alpha l + \sinh \alpha l)(\cos \alpha x - \cosh \alpha x)}{(1 + \cosh \alpha l \cos \alpha l)} \right]. \tag{q}$$

The force f might be of electrical origin, in which case it might also depend on ξ . For now we assume that the forcing function is independent of ξ , that is, that \hat{F} is a given complex constant. Then (b) provides $\xi(x, t)$.

When the denominator of (q) is zero, the response to the forcing function \hat{F} is infinite. This resonance condition results when the frequency (remember that α is determined by the frequency) is such that

$$\cos \alpha l = -\frac{1}{\cosh \alpha l}. \tag{r}$$

The solutions to this equation are the points at which the curves shown in Fig. 11.4.16 intersect. Hence the first four modes have frequencies such that αl is as shown in Table 11.4.2. Given the value of αl , the resonance frequency follows from Eq. (c)* as

$$\omega = \frac{(\alpha l)^2}{l^2} \left(\frac{Eb^3}{3\rho} \right)^{1/2}. \tag{s}$$

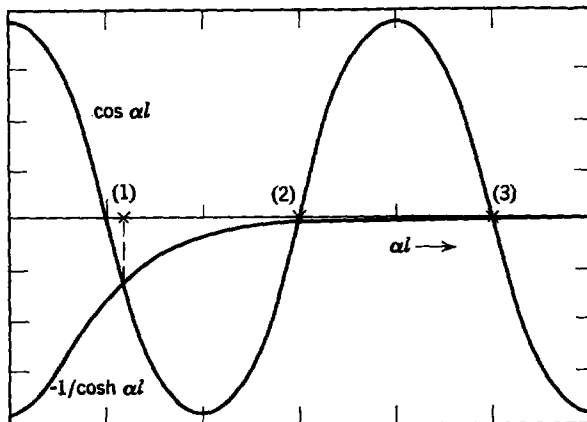


Fig. 11.4.16 Plot of the right- and left-hand sides of (r) (Example 11.4.4). The numbers indicate the solutions for the eigenvalues of the lowest three natural modes given in Table 11.4.2.

* An account of the theory of vibrating bars is given by Rayleigh in *The Theory of Sound*, 1st ed., 1877; Dover edition, 1945, p. 255, Vol. 1.

Table 11.4.2 Lowest Eigenmodes of the Beam Shown in Fig. 11.4.15a

Mode	(αl)
1	1.875
2	4.694
3	7.855
4	10.996

Note that the resonance frequency of any given mode varies inversely as the square of the beam length l , a fact that is easily verified by the experiment in Fig. 11.4.11. The numerator of (q) is plotted in Fig. 11.4.17 to show the instantaneous spatial variation of the deflection at frequencies close to the eigenfrequencies. The role played by the evanescent wave portion of the solution is clear from these deflections. In the lowest mode the deflection appears to have an “exponential” character, which indicates that the evanescent solutions dominate.

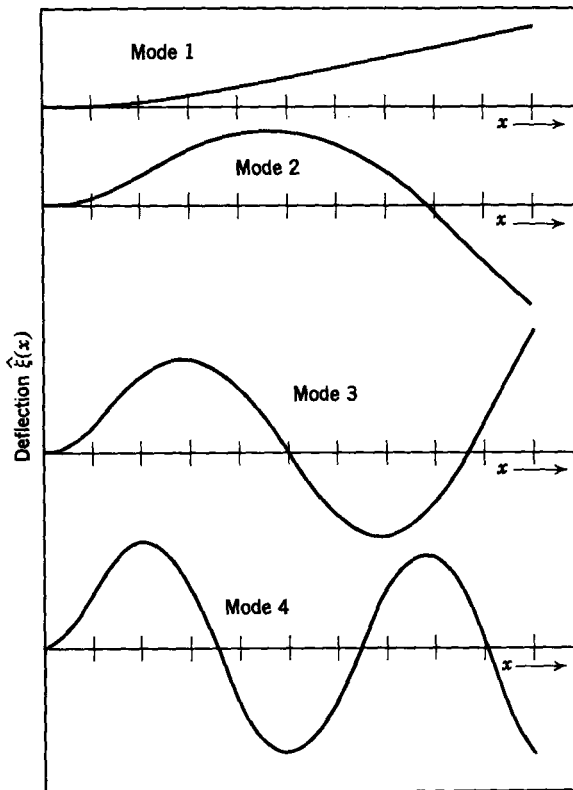


Fig. 11.4.17 Deflection of the beam as a function of the longitudinal position at an instant in time. The first four natural modes are shown, with αl as given in Table 11.4.2. The amplitude is exaggerated, with a different normalization for each mode.

By contrast the higher modes are dominated by the sinusoidal deflections of the ordinary wave solutions, with the evanescent solutions becoming apparent near the ends. This trend is also seen in Fig. 11.4.16, which shows that the higher modes (large αl) are given essentially by zeros of the function $\cos \alpha l$. These results are consistent with the notion that the evanescent waves are excited by the boundary conditions and affect only that region in the vicinity of the boundary.

The longitudinal and transverse modes considered in this section have been described in terms of quasi-one-dimensional models. As the frequency is increased, the longitudinal wavelengths take on the same magnitude as the transverse dimensions of the elastic structure. Under this condition the effect of higher order transverse modes cannot be ignored, as is illustrated in Section 11.4.3.

11.4.3 Elastic Vibrations of a Simple Guiding Structure

As mentioned in Section 11.4, the effect of boundaries is usually to couple shearing and dilatational motions of the material. As a result, the higher order modes, which become significant as the frequency is raised, are often mathematically complicated. We can, however, illustrate the basic physical effects by considering a particular class of modes composed of a purely shearing and rotational motion.*

Figure 11.4.18 shows a slab of elastic material with a thickness d . We

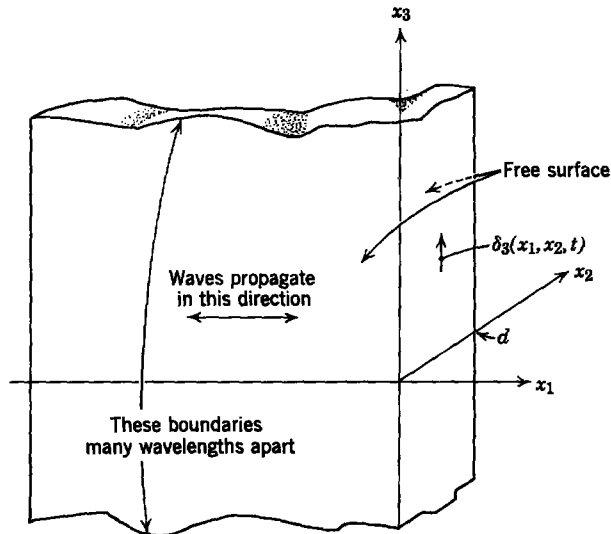


Fig. 11.4.18 Slab of elastic material with thickness d and extending to infinity in the x_3 -direction. Shearing motions of the material in the x_3 -direction are considered as they propagate in the x_1 -direction.

* For a discussion of the general modes present in elastic plates and cylinders see W. P. Mason, *Physical Acoustics*, *loc. cit.*

consider motions of the material in the x_3 -direction under the assumption that the slab has an infinite extent in the x_3 -direction. Hence displacements $\delta_3 = \delta_3(x_1, x_2, t)$ are assumed at the outset, with $\delta_1 = \delta_2 = 0$ and $\partial/\partial x_3 = 0$. These assumptions are justified if we can find solutions that satisfy (11.4.1) and the boundary conditions. The surfaces of the slab at $x_2 = 0$ and $x_2 = d$ are free; hence we require that there be no shear stresses on these surfaces:

$$T_{32}(x_1, d, t) = 0, \quad (11.4.27)$$

$$T_{32}(x_1, 0, t) = 0. \quad (11.4.28)$$

With our assumptions, (11.4.1) reduces to

$$\rho \frac{\partial^2 \delta_3}{\partial t^2} = G \left(\frac{\partial^2 \delta_3}{\partial x_1^2} + \frac{\partial^2 \delta_3}{\partial x_2^2} \right). \quad (11.4.29)$$

The boundary conditions are written in terms of δ_3 by recognizing that (11.2.32)

$$T_{32} = G \frac{\partial \delta_3}{\partial x_2}. \quad (11.4.30)$$

Except for the boundary conditions, the mathematical problem is now identical to that described in Section 10.4.1, where the two-dimensional motions of a membrane were considered; that is, (11.4.29) has a variable separable solution

$$\delta_3 = \text{Re} [X(x_1) Y(x_2) e^{j\omega t}], \quad (11.4.31)$$

and substitution shows that

$$\frac{d^2 X}{dx_1^2} + k^2 X = 0 \quad (11.4.32)$$

and

$$\frac{d^2 Y}{dx_2^2} + \alpha^2 Y = 0, \quad (11.4.33)$$

with k^2 and α^2 related by

$$k^2 + \alpha^2 = \frac{\omega^2 \rho}{G}. \quad (11.4.34)$$

The solution to (11.4.33), which satisfies the boundary conditions, is $\cos \alpha x_2$, with $\alpha = n\pi/d$, $n = 0, 1, 2, \dots$. Solutions to (11.4.32) are $e^{\pm jkx_1}$. Hence it follows that the solution (11.4.31) can be written as

$$\delta_3 = \text{Re} \cos \frac{n\pi x_2}{d} [\delta_+ e^{j(\omega t - kx_1)} + \delta_- e^{j(\omega t + kx_1)}], \quad (11.4.35)$$

where δ_+ and δ_- are complex constants determined by the longitudinal boundary conditions. For each value of n we have found solutions composed

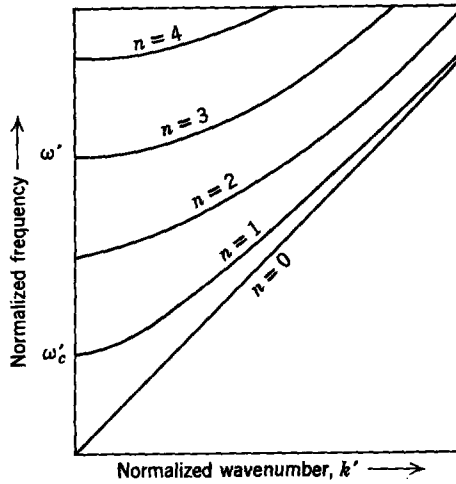


Fig. 11.4.19 Normalized frequency versus normalized wavenumber for shear modes in the elastic slab of Fig. 11.4.18: $\omega' = (\omega d/\pi)\sqrt{\rho/G}$ and $k' = kd/\pi$.

of waves that propagate along the x_1 -axis. Given the frequency ω , the wavenumber k follows from (11.4.34) as

$$k = \left[\frac{\omega^2 \rho}{G} - \left(\frac{n\pi}{d} \right)^2 \right]^{1/2}, \quad n = 0, 1, 2. \quad (11.4.36)$$

At a given frequency each of the modes has a different wavenumber and a different dependence on the transverse (x_2)-dimension. The relationship between frequency and wavenumber is shown graphically in Fig. 11.4.19. At frequencies less than $\omega' = \omega'_0$ all modes except one decay in the x_1 -direction or are evanescent in character, as we found for the membrane in Section 10.4.1. By contrast with the membrane, however, a principal mode now propagates without dispersion, even as the frequency approaches zero.

The spatial dependence of the first two modes is illustrated in Fig. 11.4.20, in which we have assumed that the frequency is below cutoff. The evanescent modes arise because of the "stiffness" introduced by the walls. The principal mode is not affected by the transverse boundary conditions, hence does not possess a cutoff frequency.

From (11.4.36) only the principal mode propagates if

$$\omega \left(\frac{\rho}{G} \right)^{1/2} < \frac{\pi}{d}. \quad (11.4.37)$$

The wavelength of the principal mode is $2\pi/k = (2\pi/\omega\sqrt{\rho/G})$; hence condition (11.4.37) can also be stated as

$$\frac{2\pi}{k} > 2d. \quad (11.4.38)$$

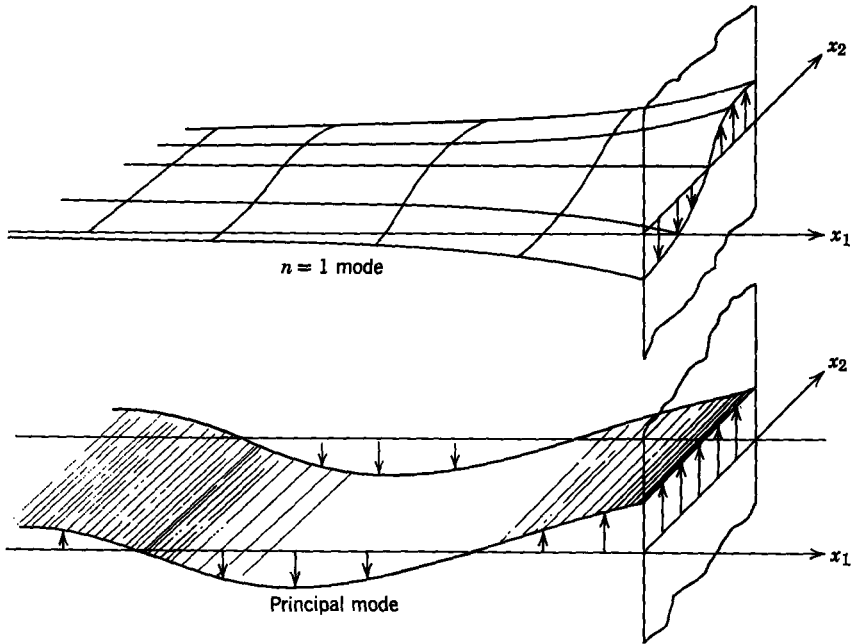


Fig. 11.4.20 Spatial distribution of the principal and $n = 1$ shear modes in an elastic slab. For the case shown the frequency is below the cutoff frequency of the $n = 1$ mode and the evanescent wave that decays in the $-x_1$ -direction is shown.

This condition illustrates the general relationship between the principal modes discussed in Section 11.4.2 and higher order modes. As long as the wavelength is long compared with the thickness, only the principal modes propagate and need be considered far from the point of excitation. As we saw in Section 10.4.1 for the membrane and in Section 11.4.2b for the thin beam, the evanescent modes are present to satisfy boundary conditions.

Modes of the kind described here are often used in delay lines. The higher modes are dispersive, hence lead to a distortion of the transmitted signal. For this reason the cutoff frequency often represents an upper limit on the frequency spectrum that can be transmitted without distortion.

11.5 ELECTROMECHANICS AND ELASTIC MEDIA

Many electromechanical interactions with elastic media can be modeled in terms of terminal pairs. This was illustrated in Chapter 9, where, even though portions of the mechanical system required continuum descriptions, the effect of electrical forces could be accounted for by means of boundary conditions. In this chapter we have confined ourselves to the three-dimensional

dynamics of elastic solids in the absence of electromechanical bulk forces. We can now readily imagine using electromechanical transducers to excite or detect the waves discussed in Section 11.4.1. At least in simple situations a discussion in this regard would parallel that given in Section 9.1.2., in which mechanical waves propagated on a thin rod. In Example 11.4.4 vibrations of an elastic beam were reduced to a terminal-pair representation that provides a convenient model for coupling to a lumped-parameter device. In a similar manner we could use a transducer to excite or detect shear waves propagating through the slab of elastic material shown in Fig. 11.4.18. By contrast, in this section we highlight a few illustrative situations in which continuum coupling with elastic media is important, but even in these cases the terminal pair concept is useful.

11.5.1 Electromagnetic Stresses and Mechanical Design

The design of electromechanical systems is often intimately concerned with material stresses produced by electromagnetic forces. A case in point is the design of large rotating machines, such as in Chapter 4. Here the energy conversion process depends on a large magnetic torque being transmitted between the rotor and stator. Because action equals reaction, the rotor and stator materials are necessarily under significant stress due to the magnetic forces; for example, this is the primary reason that conductors are placed in slots. With the conductor imbedded in a highly permeable material, the bulk of the magnetic force is on the magnetic material rather than on the conductor. If this were not the case, it would be difficult to hold the conductors down in many machines. In fact, a significant number of machine failures have been traced to fatigue of conductors and their support structures stressed by magnetic forces.

In a less obvious class of situations in which electromagnetic stresses are a major design consideration the objective is not to convert energy electromechanically. Rather the forces of electrical origin are a necessary evil. Examples in which this is the case are transformers and magnets.

In an ordinary transformer, electromechanical effects come into play in at least three mechanisms, two of which involve magnetization forces on the laminated magnetic core of the transformer. These forces arise because of inhomogeneities of the core introduced with the laminations and because of changes in the volume of the magnetic material (magnetostriction). These forces were discussed in Section 8.5.2* and are responsible for much of the noise (hum or, in transformers used for speech amplification, “transformer talk”) heard in the vicinity of an operating transformer.

A third mechanism for electromechanical effects is simply the $\mathbf{J} \times \mathbf{B}$ force density on the individual conductors in a transformer. This design consideration deserves critical attention because copper that is desirable from the point

* Summarized in Table 8.1, Appendix G.

of view of electrical conductivity tends to be lacking in mechanical strength. Transformers must be designed to withstand 25 or more times their rated currents in power applications to prevent mechanical damage under short circuit conditions. Figure 11.5.1a shows the primary and secondary windings of a distribution transformer which was intentionally subjected to currents in excess of its peak ratings. This is a step-down transformer with large

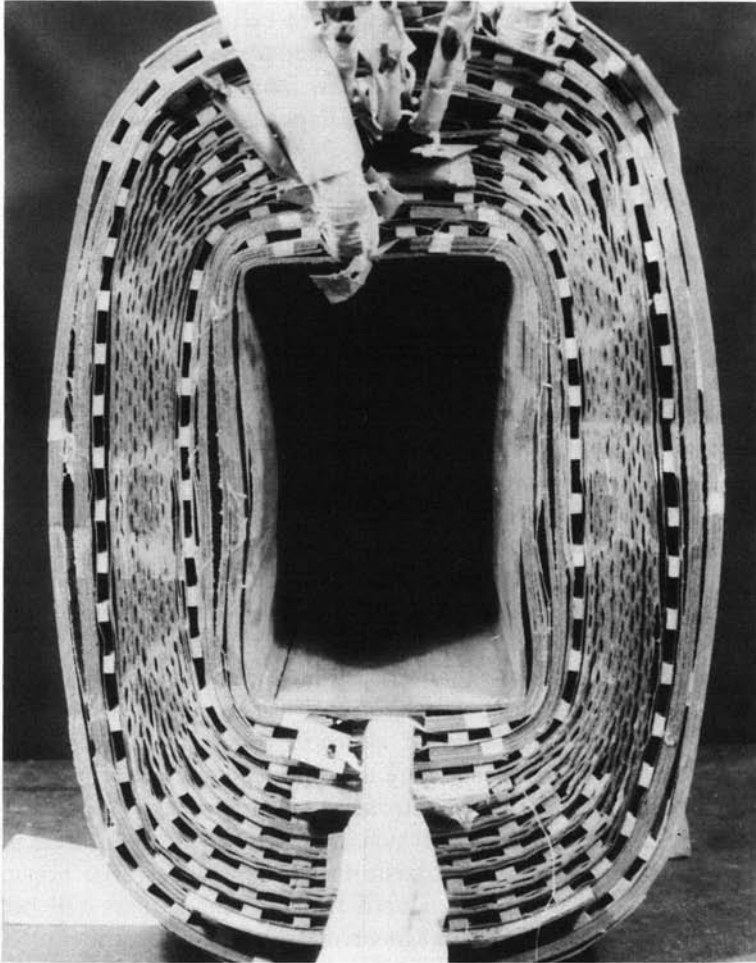


Fig. 11.5.1a End view of rectangular distribution transformer coils with core removed after being subjected to short-circuit currents in excess of design capability. Note how reaction forces on the inner secondary coil have buckled it inward on the long sides of the rectangle. Also note that forces on the outer secondary coil have rounded it outward on the long sides. Original shape of the coils on the long sides was flat. (Courtesy of the General Electric Co.)

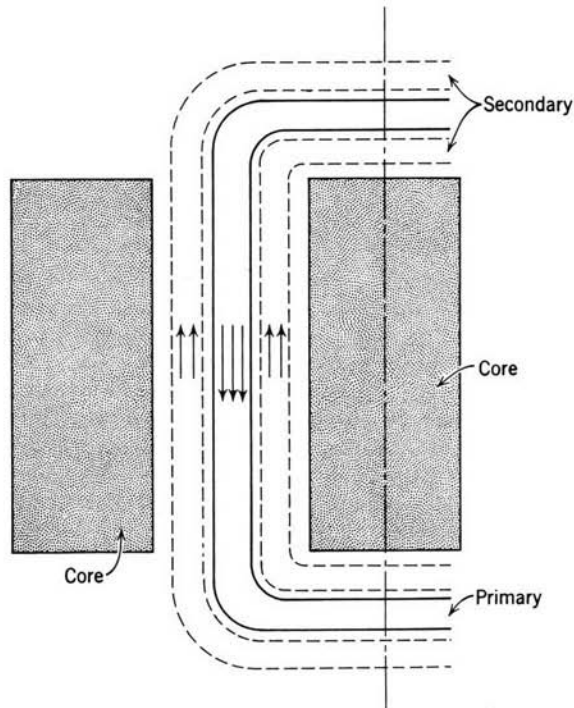


Fig. 11.5.1b Sketch of primary and secondary windings in relation to the magnetic transformer core. With the secondary short-circuited, the ampere turns in the secondary are essentially equal to those in the primary.

secondary conductors on the outside and inside and primary windings sandwiched between. The arrangement of the core and windings is sketched in Fig. 11.5.1b. The secondary windings are constructed of sheets of aluminum which were originally wound in an essentially rectangular shape. As shown in Fig. 11.5.1a, the excessive currents have distorted the secondary windings away from the primary windings. The copper secondary turns bulge inward on the inside and outward on the outside. Although, in this case, the result is not a gross mechanical failure of the structure, significant deformation of the insulation causes local damage that can lead to electrical breakdown. Also, the deformation increases the leakage reactance of the transformer. Increased leakage reactance increases regulation (voltage drops as load current increases) and this decreases the transformer efficiency, a crucial factor in distribution transformers.

So far in this chapter we have emphasized the elastic behavior of solid materials. Our main objective in this section is to draw attention to the fact that in many situations it is the *inelastic* behavior of a solid that is of interest.

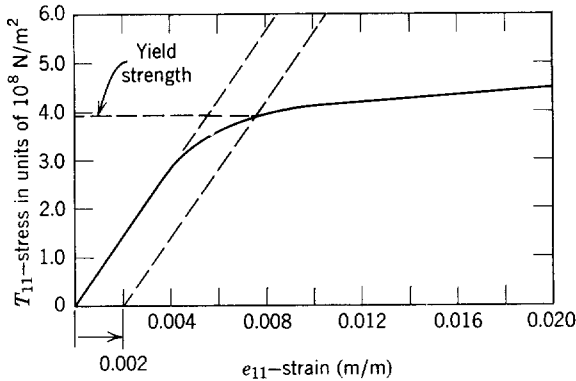


Fig. 11.5.2 Stress-strain for annealed aluminum* under tension showing definition of “yield strength” stress when limiting value of permanent strain is defined as $e_{11} = 0.002$.

If we wish to use solids to synthesize transducers, we must be careful to ensure that stresses are not so large that permanent or inelastic deformations will occur. Even more, in many situations like the one shown in Fig. 11.5.1 limiting stresses are an essential design consideration. We are then faced with the problem of defining meaningful limits on the stress that can be supported by the material. Because the inelastic behavior is an upper bound on the elastic deformation of the material, we can use the elastic theory developed in earlier sections as a starting point for computing limiting stresses.

A typical stress-strain relation for a polycrystalline metal is shown in Fig. 11.5.2. For small values of the stress and strain the relationship is essentially linear. As the stress is raised, however, a point is reached at which the resulting material strain increases more rapidly. Above this point, if the material is unloaded, it is likely that it will retain a permanent deformation. An index of the degree of this permanent set is the *yield strength* of the material, which is defined in Fig. 11.5.2. After the material has been loaded to the yield strength (the limiting stress) it is *assumed* that if it were unloaded it would return to the zero stress condition along a straight line parallel to the loading curve in the elastic range. To fix the yield strength of a material we must define the hypothetical permanent set (the strain) taken by the material when the stress is returned to zero. (In practice this might be 0.002 for metals in tension.*)

If the material has an elastic regime, it is possible to obtain an approximate prediction of material stresses that will lead to inelastic behavior by first predicting the stresses by means of the elastic model and then comparing the maximum stress to the yield strength. Generally such calculations are used to

* See S. H. Crandall and N. C. Dahl, *An Introduction to the Mechanics of Solids*, McGraw-Hill, New York, 1959, p. 173.

compute an upper bound on loading the material, with a margin of safety included in the design. The following example illustrates this procedure.

Example 11.5.1. In this example we illustrate how the simple model of an elastic beam can be used to provide insight into the limiting stresses that can be supported by current-carrying conductors in the situation illustrated in Fig. 11.5.1. We assume that the primary winding (sandwiched between the two secondary windings) will remain essentially rigid but that the secondary windings can be modeled by thin beams of the nature discussed in Section 11.4.2*b*. The problem then reduces to that illustrated in Fig. 11.5.3*a*, in which only the secondary conductors to the right of the primary are shown.

Under short circuit conditions the ampere turns in the secondary and primary are essentially equal. This means that the magnetic field between the conductors is essentially uniform and given by

$$H = \frac{I}{2w}, \quad (a)$$

for only half the secondary ampere turns are in the part of the windings shown in Fig. 11.5.3*a*.

For simplicity we assume that the section of secondary conductor can be considered as being clamped at $x_1 = 0$ and $x_1 = l$. Hence we have as boundary conditions

$$\xi(0) = 0; \quad \xi(l) = 0, \quad (b)$$

$$\frac{d\xi}{dx_1}(0) = 0; \quad \frac{d\xi}{dx_1}(l) = 0. \quad (c)$$

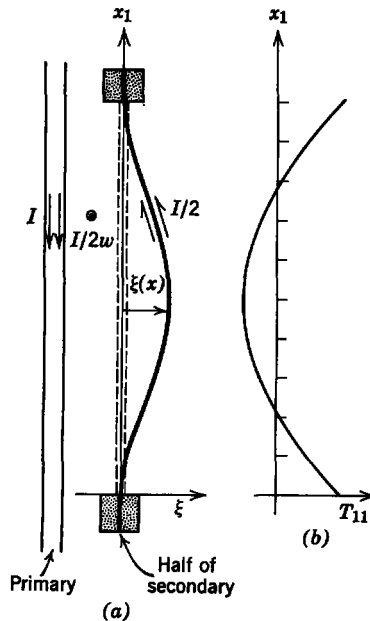


Fig. 11.5.3 (a) A simple model is used to predict elastic failure of the sheet secondary conductor. This example is a first approximation to the situation in Fig. 11.5.1; the primary is assumed to be rigid and the system has a width w into the paper. (b) Distribution of longitudinal stress T_{11} evaluated on the inside surface of the secondary.

Of course, in a transformer the currents, hence the magnetic forces, are not constant. In a distribution transformer the current alternates at 60 Hz, and the magnetic forces that depend on the square of the current are therefore composed of constant and second harmonic (120-Hz) parts. Now the conductors can respond, transducer fashion, to the alternating component of the $\mathbf{J} \times \mathbf{B}$ force.* Here, however, we are interested only in the deformations of the conductors that result over many cycles of the current. Hence we regard the magnetic force on the conductors as being constant and having its average value. Because this force varies as the square of the current, it amounts to using the rms value of the current in evaluating the magnetic force on the secondary conductors. In what follows it is assumed that I is the total rms ampere turns through the width w of the primary conductors.

Under steady conditions (11.4.26), which expresses the transverse force balance for the secondary conductors modeled as a single elastic beam, becomes

$$\frac{d^4 \xi}{dx_1^4} = \frac{3}{2b^3 E} T_2. \quad (d)$$

Here $2b$ is the thickness of the combined secondary conductors, E is the "equivalent" modulus of elasticity based on the combined conductors and insulation, and T_2 is the force per unit area acting in the transverse direction. Given T_2 , it is a simple matter to compute the deflection ξ of the beam model.

It follows from the magnetic stress tensor† that the surface force T_2 is constant and that

$$T_2 = \frac{1}{2} \mu_0 \left(\frac{I}{2w} \right)^2, \quad (e)$$

which combines with (d) to provide a simple fourth-order ordinary equation that can be integrated directly:

$$\frac{d^4 \xi}{dx_1^4} = a, \quad (f)$$

where

$$a = \frac{3\mu_0}{4b^3 E} \left(\frac{I}{2w} \right)^2.$$

Four succeeding integrations lead to a solution that involves four constants $C_1 \cdots C_4$.

$$\xi = \frac{ax_1^4}{24} + \frac{C_1 x_1^3}{6} + \frac{C_2 x_1^2}{2} + C_3 x_1 + C_4. \quad (g)$$

From boundary conditions (b) and (c) these constants are evaluated to obtain

$$\xi = \frac{al^4}{24} \left(\frac{x_1}{l} \right)^2 \left(\frac{x_1}{l} - 1 \right)^2 \quad (h)$$

for the deflection as a function of the longitudinal position x_1 . This is the deflection plotted in Fig. 11.5.3a.

So far our calculations have been based on an elastic model for the beam. The objective is to determine the values of the current that lead to permanent deformations of the secondary winding. This is done by evaluating the maximum longitudinal stress T_{11} and comparing it to that required to give elastic failure of the material according to the preceding discussions of this section.

* In fact, under conditions of extreme loading the conductors of a large transformer can be seen to "breathe" in and out at 120 Hz.

† See Table 8.1 of Appendix G.

Remember that the longitudinal stress varies linearly over the cross section of the beam (e.g., see Fig. 11.4.14). In the thin beam model this stress is related to the deflection by (11.4.18), which becomes

$$T_{11} = -x_2 E \frac{d^2 \xi}{dx_1^2} = \frac{-x_2 E a l^2}{2} \left[\left(\frac{x_1}{l} \right)^2 - \left(\frac{x_1}{l} \right) + \frac{1}{6} \right], \quad (i)$$

where x_2 is the transverse coordinate. The maximum stress is obtained at the beam surfaces, where $x_2 = \pm b$; for example, on the inside (left) surface of the beam

$$T_{11} = \left(\frac{l}{b} \right)^2 \frac{3}{8} \mu_0 \left(\frac{l}{2w} \right)^2 \left[\left(\frac{x_1}{l} \right)^2 - \left(\frac{x_1}{l} \right) + \frac{1}{6} \right]. \quad (j)$$

The manner in which this function depends on the longitudinal position is shown in Fig. 11.5.3*b*. At the center of the beam ($x_1 = l/2$) the stress $T_{11}(x_2 = -b)$ is negative, indicating that the material is under compression. The maximum longitudinal stress is obtained at the ends, where the material on the left side of the beam is under tension. This maximum stress on the beam is

$$T_{11}(x_2 = -b, x_1 = 0) = \left(\frac{l}{b} \right)^2 \frac{1}{16} \mu_0 \left(\frac{l}{2w} \right)^2. \quad (k)$$

Now the beam is also subject to shear stresses T_{12} , which should also be considered in determining the maximum stress. The shear stress is related to the beam deflection by (11.4.21), which shows that if $b \ll l$ the shear stress will be small compared with the longitudinal stress. It is just this fact that the beam is thin that makes the mechanical stress T_{11} much greater than the magnetic pressure. The stress T_{11} acts over the cross section $2b$ of the beam through a lever arm that is less than b to hold in equilibrium the magnetic pressure $\frac{1}{2} \mu (l/2w)^2$ acting over the length l through a lever arm that is on the order of l (see Fig. 11.4.13). This is why (k) is proportional to the magnetic pressure amplified by $(l/b)^2$.

An order of magnitude calculation helps us to appreciate the significance of (k). In magnetic circuits, such as the transformer of Fig. 11.5.1, a magnetic flux density of 10 kG (1 Wb/m^2) is commonly induced. This corresponds to a magnetic pressure of

$$\frac{B^2}{2\mu_0} = \frac{1}{(2)(4\pi \cdot 10^{-7})} \approx 4 \cdot 10^5 \text{ N/m}^2.$$

If we use this number to replace the magnetic pressure $\frac{1}{2} (l/2w)^2 \mu_0$ in (k) and let $l/b = 20$, it follows that

$$T_{11}(x_2 = -b, x_1 = 0) = 2 \cdot 10^7 \text{ N/m}^2.$$

This is just above the 0.2% yield strength of annealed aluminum,* but considerably below the value in Fig. 11.5.2. The strength of aluminum can be increased considerably by cold working and alloying it with other substances. For example, considering the ability of the coil to withstand the mechanical forces imposed by short-circuit currents, a transformer designer is faced with the problem of balancing the mechanical strength of the core and coil against the cost and electrical characteristics. His problem is complicated because coil conductors that are most desirable in terms of their electrical characteristics are relatively low in mechanical strength.

A critical review of this model will show that we have ignored many facets of the problem that could be of major importance; for example, the secondary winding of the actual transformer is not a homogeneous solid but rather is composed of layers of conducting and

* A. E. Knowlton, *Standard Handbook for Electrical Engineers*, McGraw-Hill, New York, 1957, Section 4, p. 695.

insulating sheets. In practice we would probably measure an "equivalent" modulus of elasticity for this combination, although to be rigorous account should be taken of the anisotropic material in the basic model of the elastic beam.

Also, the inelastic behavior of materials is more complicated than might be deduced from our comments so far. The material is subject to repeated loading and unloading due to the second-harmonic force. This can result in a type of failure analogous to that found when a wire is bent back and forth repeatedly until it breaks. It depends on the number of cycles as well as the maximum stress and is therefore referred to as *fatigue* failure.

To complicate the picture still further, when materials are subjected to a constant stress over a long period of time, it is found that the strain has an initial value that can be predicted from the stress-strain relation but continues to increase with time. This *creep* phenomenon can eventually lead to the failure of the material. Copper is an example of a material that displays creep. Further discussion of the inelastic behavior of materials is beyond the scope of this book but should be recognized as required for the understanding of how materials are used in electromechanical systems.

11.5.2 Simple Continuum Transducers

This chapter is concluded with examples that show how quasi-one-dimensional models of elastic structures can be used in the design of electro-mechanical transducers.

11.5.2a Variable Capacitance Coupling

We begin with a situation that involves an electromechanical coupling similar to that studied back as far as Chapter 3—variable capacitance coupling. The object is to develop a simple and reliable low-frequency notch filter. It is required that the frequency of the notch be tuned by varying a voltage.

Example 11.5.2. An electromechanical filter, having as its basic element a simple cantilevered beam, is shown in Fig. 11.5.4. The beam, which is at the potential V_o , is free to vibrate between plane-parallel electrodes, and the input signal is imposed on the left electrode. Because v_i is much less than V_o , this produces a force on the beam proportional to the input signal. The beam deflections lead to a change in capacitance between the beam and the plate to the right. The resulting current through the resistance R is therefore proportional to the input signal with an amplitude determined by the response of the beam to the input.

It is assumed that the resistance R is small enough that the electrode to the right can be considered as grounded. Further, it is assumed that the capacitive reactance due to C is small compared with R , so that v_o can be taken as the voltage drop across the resistance.

The equation of motion for the beam is (11.4.26):

$$\frac{\partial^2 \xi}{\partial t^2} + \frac{Eb^2}{3\rho} \frac{\partial^4 \xi}{\partial x_1^4} = \frac{T_2}{2b\rho}. \quad (a)$$

We assume that $d \ll l$ so that the transverse force T_2 is simply the difference in Maxwell stress* acting on the opposite surfaces of the beam:

$$T_2 = T_{22}^a - T_{22}^b = \frac{1}{2}\epsilon_0 \left[\frac{(V_o + v_i)^2}{(d - \xi)^2} - \frac{V_o^2}{(d + \xi)^2} \right]. \quad (b)$$

* Table 8.1, Appendix G.

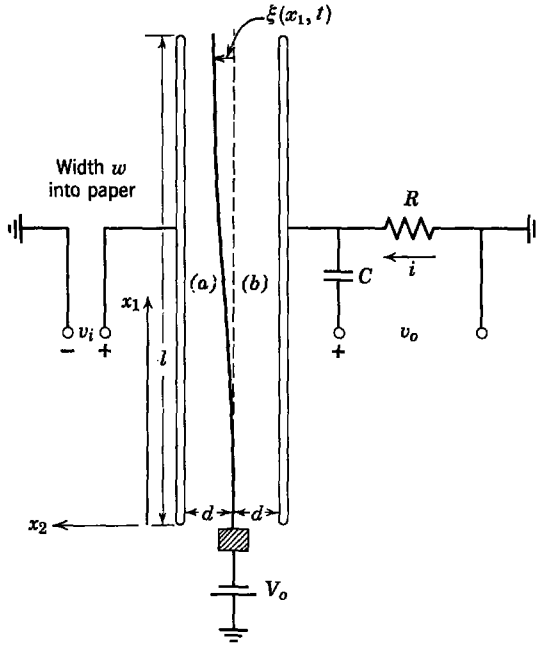


Fig. 11.5.4 A cantilevered beam has the potential V_o relative to plane-parallel driving and detecting electrodes. This device might be used as a low-frequency voltage tunable electro-mechanical filter.

For small deflections ξ and input voltage v_i this becomes

$$T_2 = 2\epsilon_0 \left(\frac{V_o}{d} \right)^2 \frac{\xi}{d} + \frac{\epsilon_0 V_o}{d^2} v_i. \tag{c}$$

The equation of motion (a) is then augmented by two additional forces, one having the nature of a spring with a negative spring constant and the other a driving force proportional to the driving voltage:

$$\frac{\partial^2 \xi}{\partial t^2} + \frac{Eb^2}{3\rho} \frac{\partial^4 \xi}{\partial x_1^4} = \frac{\epsilon_0 V_o^2}{b\rho d^3} \xi + \frac{\epsilon_0 V_o}{2b\rho d^2} v_i. \tag{d}$$

We confine attention to the sinusoidal steady-state response of the system and so assume that the drive and response have the form

$$\begin{aligned} v_i &= \text{Re } \hat{v}_i e^{j\omega t}, \\ \xi &= \text{Re } \hat{\xi}(x_1) e^{j\omega t}. \end{aligned} \tag{e}$$

Then (d) becomes

$$\frac{d^4 \hat{\xi}}{dx_1^4} - \alpha^4 \hat{\xi} = P \hat{v}_i, \tag{f}$$

where

$$\alpha^4 = \left[\frac{\epsilon_0 V_o^2}{d^3 b \rho} + \omega^2 \right] \frac{3\rho}{Eb^2}$$

$$P = \frac{3}{2} \frac{\epsilon_0 V_o}{d^2 b^3 E}.$$

This inhomogeneous ordinary equation has a homogeneous solution which is identical in form to that studied in Example 11.4.4 of Section 11.4.2*b*. In addition, there is now an inhomogeneous solution which, because the right-hand side of (f) is a constant, is simply a constant. The complete solution is

$$\xi = A \sin \alpha x_1 + B \cos \alpha x_1 + C \sinh \alpha x_1 + D \cosh \alpha x_1 - \frac{P \hat{v}_i}{\alpha^4}. \quad (g)$$

The boundary conditions on the beam which determine the constants A , B , C , and D require that the clamped end of the beam be constrained so that no longitudinal or transverse displacement is there and that the free end of the beam at $x_1 = l$ is free of shear and longitudinal stress. In terms of the transverse displacement ξ of the beam, these conditions are

$$\begin{aligned} \xi(0) &= 0; & \frac{d^2 \xi}{dx_1^2}(l) &= 0, \\ \frac{d \xi}{dx_1}(0) &= 0; & \frac{d^3 \xi}{dx_1^3}(l) &= 0. \end{aligned} \quad (h)$$

These conditions require that the following four simultaneous equations be satisfied:

$$\begin{aligned} A(0) + B(1) + C(0) + D(1) &= P \hat{v}_i / \alpha^4, \\ A(1) + B(0) + C(1) + D(0) &= 0, \\ A(-\sin \alpha l) + B(-\cos \alpha l) + C(\sinh \alpha l) + D(\cosh \alpha l) &= 0, \\ A(-\cos \alpha l) + B(\sin \alpha l) + C(\cosh \alpha l) + D(\sinh \alpha l) &= 0. \end{aligned} \quad (i)$$

The constants A , B , C , and D follow from these equations and the deflection of the beam is now known.

To compute the output voltage it is necessary first to recognize that the surface charge density on the right plate is

$$\sigma_f(x_1, t) = \frac{\epsilon_0 V_o}{d + \xi} \approx \frac{\epsilon_0 V_o}{d} - \frac{\epsilon_0 V_o \xi}{d^2} \quad (j)$$

Then it follows that because the current through the resistance is the time rate of change of the total charge on the plate to the right

$$\hat{v}_o = -Ri = j\omega R \frac{w \epsilon_0 V_o}{d^2} \int_0^l \xi dx_1. \quad (k)$$

It is a straightforward matter to carry out this integration, since ξ is given by (g). Note from (i) that each of the constants is proportional to \hat{v}_i and inversely proportional to the determinant of the coefficients $\Delta(\omega)$. Hence (k) for the transfer response has the form

$$\hat{v}_o = \frac{H(\omega)}{\Delta(\omega)} \hat{v}_i, \quad (l)$$

and the poles of the transfer function are given by

$$\Delta(\omega) = 0. \quad (\text{m})$$

These are the same poles found for the beam in Example 11.4.4; that is, the determinant of the coefficients is zero if (remember $\alpha = \alpha(\omega)$)

$$1 + \cosh \alpha l \cos \alpha l = 0. \quad (\text{n})$$

The roots of this expression are given in Table 11.4.2.

If we call the roots of (n) $(\alpha l)_n$, it follows that the resonance frequencies are given by

$$\omega = \pm \left(\omega_n^2 - \frac{\epsilon_0 V_o^2}{d^3 b \rho} \right)^{1/2}, \quad (\text{o})$$

where

$$\omega_n = \frac{(\alpha l)_n^2}{l^2} \left(\frac{E b^3}{3 \rho} \right)^{1/2} \quad (\text{p})$$

are the resonance frequencies of the beam without electromechanical coupling. At the frequencies given by (o) there is a resonance in the transfer function unless $H(\omega)$ happens to be zero. Note that these resonance frequencies can be tuned by varying the voltage V_o . As we might have expected at the outset, (o) shows that the beam has an unstable equilibrium at $\xi = 0$ when the lowest resonance frequency is reduced to zero and these lowest eigenfrequencies become imaginary. From (o) the condition for instability is

$$\frac{\epsilon_0 V_o^2}{d^3 b \rho} = \omega_1^2. \quad (\text{q})$$

11.5.2b Magnetostrictive Coupling

The subject of magnetostriction in solids is sufficiently complex that a comprehensive treatment is inappropriate here. We can, however, gain a considerable qualitative insight into the subject by considering one-dimensional motions of a thin rod subject to magnetostrictive forces. In this context these forces can be viewed as described by the force density developed in Section 8.5.2.* There are two reasons why the force density developed in Chapter 8 is not entirely adequate. First of all, there is no guarantee that a solid remains isotropic after a magnetic field is applied, even though it may be isotropic in the absence of a magnetic field. Second, solids that exhibit significant magnetostrictive behavior tend to be magnetic; for example nickel and nickel iron alloys are commonly used in magnetostrictive transducers.† In these materials \mathbf{B} is a linear function of \mathbf{H} only over a limited range of \mathbf{H} . Hence the permeability μ relates \mathbf{B} and \mathbf{H} only so long as \mathbf{B} is much less than its saturation value.

By limiting ourselves to one-dimensional motions and sufficiently small magnetic field intensities that $\mathbf{B} = \mu \mathbf{H}$ we can use the results of Chapter 8

* Table 8.1, Appendix G.

† A discussion of magnetostriction, including material characteristics and applications to the design of electronic devices is given in W. P. Mason, *Electromechanical Transducers and Wave Filters*, Van Nostrand, Princeton, New Jersey, 1958, 2nd. ed., p. 215.

to gain a meaningful understanding of the basic magnetostrictive interaction. Actually, most transducers are modeled as one-dimensional, and nonlinear effects are accounted for empirically by straightforward extensions of the linear model.

As discussed in Section 8.5, we can think of magnetostrictive interactions as resulting because dilatational motions of the material, which lead to local changes in the material density, also lead to a change in the local magnetic energy storage. This makes it possible to exert a magnetic force on a volume where material is initially homogeneous. An example in which this is a desirable attribute is given in Fig. 11.5.5a. There, a magnetic wire constitutes the propagating structure for an acoustic delay line. The device, which might be used as either an input or an output transducer, is easily moved along the wire to effect a change in the delay time. Now, if the wire were capable of only rigid body motion, there could be no longitudinal force produced by the input signal. The material must change its volume in order to effect any change in the magnetic energy stored in the system as a function of material displacements. This should be contrasted with the type of magnetization

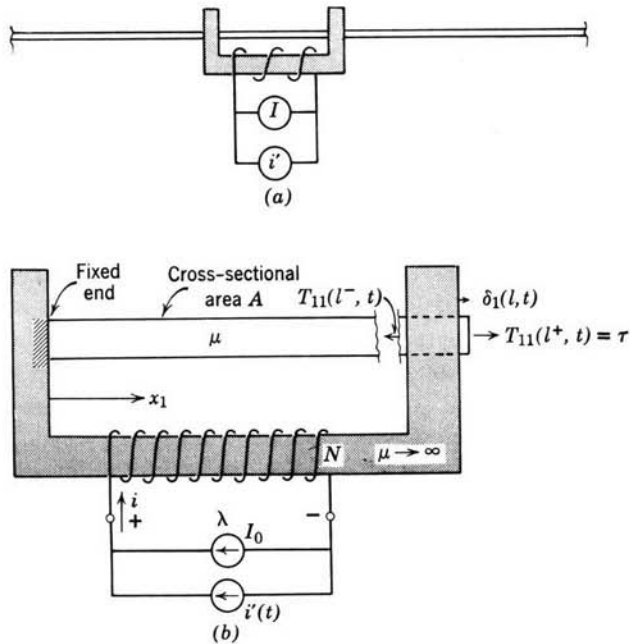


Fig. 11.5.5 Magnetostrictive transducer. Compressional motions are excited by the input current $i'(t)$: (a) transducer placed at a variable position along a magnetic wire which might be used as a delay line; (b) detail of a transducer in which the wire is fixed at one end of a magnetic circuit.

forces used in the delay line of Section 9.1.2, where the force resulted because of inhomogeneities (air gaps) in the material. The inconvenience of this mode of coupling is made apparent in Figure 9.1.14.

The following example illustrates the modeling of a magnetostrictive transducer.

Example 11.5.3. The transducer shown in Fig. 11.5.5*b* characterizes devices that have seen wide application. An input signal $i'(t)$ is transduced into a force τ that acts through a displacement $\delta_1(l, t)$, we wish to find the mechanical terminal relation between τ and $\delta_1(l, t)$. To simplify our discussion, it is assumed that the magnetostrictive material takes the form of a rod with cross-sectional area A and one end fixed at $x_1 = 0$.

According to (8.5.38), the rod is subject to the force density

$$\mathbf{F} = -\frac{1}{2}\mathbf{H} \cdot \mathbf{H} \nabla \mu + \nabla \left(\frac{1}{2}\mathbf{H} \cdot \mathbf{H} \frac{\partial \mu}{\partial \rho} \right) \quad (\text{a})$$

In the rod it is reasonable to view μ and ρ as being uniquely related, $\mu = \mu(\rho)$. Note that if a material is inhomogeneous this is not a meaningful statement; for example, a material could have a uniform density but be composed of regions occupied by materials of different permeabilities μ . On the basis of the restriction that the force is valid only in the interior of the rod so that $\mu = \mu(\rho)$, we can write

$$\nabla \mu = \frac{\partial \mu}{\partial \rho} \nabla \rho. \quad (\text{b})$$

Then (a) reduces to

$$\mathbf{F} = \rho \nabla \left(\frac{1}{2} \frac{\partial \mu}{\partial \rho} \mathbf{H} \cdot \mathbf{H} \right). \quad (\text{c})$$

In what follows we make the assumption that insofar as the force is concerned variations in ρ can be ignored so that the mass density multiplying the gradient term in (c) is replaced by ρ_0 . Note that this does not say that ρ is actually a constant, but simply that it can be approximated as constant in (c). Then the longitudinal equation of motion for the rod becomes

$$\rho_0 \frac{\partial^2 \delta_1}{\partial t^2} = \frac{\partial}{\partial x_1} \left(E \frac{\partial \delta_1}{\partial x_1} + \frac{\rho_0}{2} \frac{\partial \mu}{\partial \rho} \cdot \mathbf{H} \right). \quad (\text{d})$$

It is a good approximation to ignore the effect of mechanical deformation on the field. This means that \mathbf{H} is uniform over the length of the rod between $x_1 = 0$ and $x_1 = l$. Over this range, material displacements are then governed by the simple wave equation for the thin rod

$$\frac{\partial^2 \delta_1}{\partial t^2} = \left(\frac{E}{\rho_0} \right)^{1/2} \frac{\partial^2 \delta_1}{\partial x_1^2}. \quad (\text{e})$$

The influence of the magnetostrictive force is felt through the boundary condition at $x_1 = l$. Force equilibrium for a section of the rod in the neighborhood of $x_1 = l$ is shown in Fig. 11.5.6.

The quantity in brackets on the right-hand side of (d) is the longitudinal stress transmitted along the rod. Hence the left face of the section of material shown in Fig. 11.5.6 is subject to this stress acting over the cross section A of the rod. Within the length h of the material section the lines of magnetic field intensity are shunted into the magnetic circuit. The stress on the right surface is simply τA , where τ is the mechanical stress due to the system

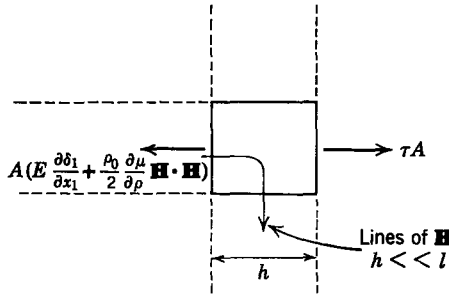


Fig. 11.5.6 A section of the rod shown in Fig. 11.5.5 in the neighborhood of $x_1 = l$. This section is assumed to have negligible length h compared with l .

being driven. We can argue that there are no shear stresses acting on the volume by recognizing from (c) that the magnetostriction force is capable only of producing normal stresses. Hence at $x = l$,

$$E \frac{\partial \delta_1}{\partial x_1}(l, t) + \rho_0 \frac{1}{2} \frac{\partial \mu}{\partial \rho} \mathbf{H}^2(l, t) = \tau. \tag{f}$$

This becomes a useful boundary condition once \mathbf{H} is evaluated in terms of the current i . For illustrative purposes we assume that the magnetic circuit is of much greater permeability than the magnetostrictive wire. Then

$$H = \frac{Ni}{l} = \frac{N}{l} (I_0 + i'). \tag{g}$$

The force equilibrium represented by (f) has a constant part due to the bias current I_0 and a dynamic part due to small perturbations $i'(t)$ in the transducer current. We assume that the constant part is balanced out by a constant part of τ due to the system to the right. Then the linearized dynamic part of (f) is

$$\frac{\partial \delta'}{\partial x_1}(l, t) + \gamma i' = \frac{\tau'}{E}, \quad \text{where } \gamma = \frac{\rho_0}{E} \frac{\partial \mu}{\partial \rho} \left(\frac{N}{l}\right)^2 I_0, \tag{h}$$

and τ' and δ' are, respectively, the time-varying parts of the stress acting on the right surface of the transducer rod and displacement $\delta_1(x_1, t)$.

Our objective is to characterize the transducer by the relation between τ' and $\delta'(l, t)$, given the input signal $i'(t)$. This is easily accomplished for sinusoidal steady-state solutions in the form of

$$\begin{aligned} i' &= \text{Re } i e^{j\omega t}, \\ \delta' &= \text{Re } \delta(x_1) e^{j\omega t}, \\ \tau' &= \text{Re } \hat{\tau} e^{j\omega t} \end{aligned} \tag{i}$$

by recognizing that the solution to (e), which satisfies the condition that there be no displacement at $x_1 = 0$, is

$$\delta = C \sin kx_1, \quad k = \omega \left(\frac{\rho_0}{E}\right)^{1/2}. \tag{j}$$

The complex amplitudes of (i) must satisfy a further condition represented by (h),

$$Ck \cos kl + \gamma i = \frac{\hat{\delta}}{E}. \quad (\text{k})$$

Finally, it follows from (j) that $C = \delta(l)/\sin kl$ and that this last expression becomes the required terminal relation between the mechanical variables $\delta'(l, t)$ and $\tau'(t)$ and the driving signal $i'(t)$.

$$\gamma i = \frac{\hat{\delta}}{E} - \delta(l)k \cot kl. \quad (\text{l})$$

This terminal relation is all that is required to represent the magnetostrictive transducer as it affects the medium being driven; for example, if the transducer were used to drive a rod to the right (l) would constitute a boundary condition to be used at $x_1 = l$.

The constant γ can be positive or negative depending on the properties of the rod. As made familiar by preceding chapters, the transducer has a linear response only if it is biased by an external source such as I_0 .

11.5.2c Piezoelectric Coupling

A salient feature of all the mechanisms for electromechanical coupling so far discussed has been that electromagnetic forces depend on the square of the applied currents, potentials, or other electrical excitations. This has meant that to obtain an electromagnetic force proportional to the applied signal a bias field is required. It has also been necessary to provide a bias field in situations in which a mechanical motion is to be transduced into an electrical signal. The magnetostrictive interaction discussed in Section 11.5.2b illustrates this point. The bias current I_0 is required to make the force a linear function of the input signal $i'(t)$. This bias current is also required if the transducer is to be used to detect the motion of the magnetized rod, as, for example, at the output end of a delay line.

Piezoelectric and piezomagnetic forms of electromechanical coupling are of interest because in effect they provide their own internal bias. The dielectric bar shown in Fig. 11.5.7 is an example of a piezoelectric transducer. That there are new ingredients to this physical situation is apparent from two simple experiments. First, suppose that a voltage is applied between the upper and lower electroded surfaces of the bar. The result is an expansion or contraction of the bar in the x -direction, depending on the sign of the applied voltage. The mechanical response reflects the sign of the applied signal. Second, suppose that the bar is stretched or compressed along the x -axis. A proportionate voltage will be developed across the terminals. These electrical-to-mechanical and mechanical-to-electrical effects are similar to those found in a transducer with an internal bias. In piezoelectric materials the effect of the bias is intrinsic to the material.

Materials that display piezoelectric properties can be either single crystals, for example, quartz, or polycrystalline ferroelectrics such as barium titanate ceramics. In the latter materials the "bias" referred to previously is provided

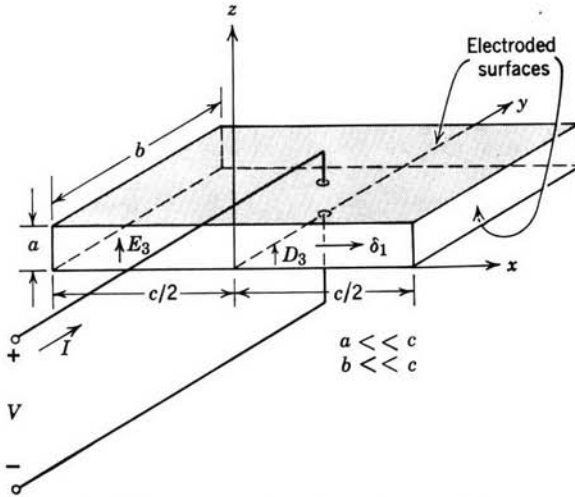


Fig. 11.5.7 Piezoelectric length expander bar.

by a permanent polarization. In single crystals the piezoelectric phenomenon is brought about by asymmetry in the crystal structure. In general, this subject therefore involves the elastic and electrical behavior of anisotropic solids. In the following introduction to this class of electromechanical interaction attention is confined to a particular one-dimensional type of interaction which allows us to develop some insight into the subject without becoming involved with general statements about the dynamics of anisotropic media.*

As might be imagined from the analogy between the piezoelectric transducer and the biased transducer, it is impossible to distinguish between electrical and mechanical forces in piezoelectric materials. If we refer to the total stress in the material as T_{11} , the electrical constitutive law relating D_3 and E_3 is

$$D_3 = \epsilon E_3 + \gamma T_{11}. \quad (11.5.1)$$

Here we have confined attention to quasi-one-dimensional motions of the bar along the x -axis and a crystal configuration such that the induced electric field is in the z -direction. Thus

$$\delta = \delta_1(x, t)\mathbf{i}_1, \quad \mathbf{E} = E_3(x, t)\mathbf{i}_3. \quad (11.5.2)$$

The mechanical constitutive law, which represents a generalization of the stress-strain relation, is

$$e_{11} = \gamma E_3 + ST_{11}. \quad (11.5.3)$$

* For a more general discussion, see W. P. Mason, *Physical Acoustics* Vol. 1, part A, Academic, New York, 1964 p. 170.

The parameter S will be recognized as the reciprocal of the modulus of elasticity. Note that the same constant γ appears in (11.5.1) and (11.5.3) to account for the electromechanical coupling. This is a consequence of a reciprocity condition, based on conservation of energy in much the same spirit discussed in Section 3.1.2c. To see this consider a section of the bar with length Δx which is subject to a slowly varying stress T_{11} , as shown in Fig. 11.5.8. T_{11} is the total stress (mechanical plus electrical), hence for slow variations it is constant over the length Δx of the section. The work done on the sample as it undergoes the incremental displacement $d\delta_1$ is

$$ab[T_{11} d\delta_1(x + \Delta x) - T_{11} d\delta_1(x)] \simeq abT_{11} \Delta x d\left(\frac{\partial\delta_1}{\partial x}\right) = abT_{11} \Delta x de_{11}. \quad (11.5.4)$$

Energy can also be added to the sample through the electrical terminals. The charge on the upper electrode is $q = -\Delta x b D_3$ and the voltage between the electrodes is $-aE_3$. A change in the charge dq on the upper plate corresponds to an addition of energy through the electrical terminals given by

$$v dq = ab \Delta x E_3 dD_3. \quad (11.5.5)$$

It is now possible to write a conservation of energy equation by defining the energy density (mechanical and electrical) within the element as w :

$$ab \Delta x E_3 dD_3 + ab \Delta x T_{11} de_{11} = ab \Delta x dw \quad (11.5.6)$$

or

$$E_3 dD_3 + T_{11} de_{11} = dw. \quad (11.5.7)$$

Note that the thermodynamic subsystem described by this conservation of energy equation includes energy storage in the elastic deformation of the material. This is necessary because we cannot distinguish between mechanical and electrical stresses as we can in Chapter 3, where we consider forces f^e that are zero with the electrical terminals unexcited. It is appropriate to think of D_3 and e_{11} in (11.5.7) as thermodynamically independent variables. This representation is similar to that used in Chapter 3, in which D_3 would be the charge q and e_{11} would be the mechanical displacement. To make E_3 and T_{11} (which are analogous to the voltage and force) the independent variables we use Legendre's dual transformation (see Section 3.1.2b) to write (11.5.7) as

$$D_3 dE_3 + e_{11} dT_{11} = dw', \quad (11.5.8)$$

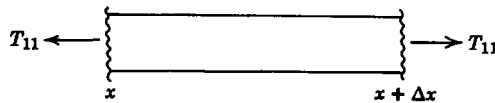


Fig. 11.5.8 Incremental length of bar shown in Fig. 11.5.7.

where the coenergy density w' is defined as

$$w' = E_3 D_3 + T_{11} e_{11} - w. \quad (11.5.9)$$

Because $w' = w'(E_3, T_{11})$, we can also write

$$\frac{\partial w'}{\partial E_3} dE_3 + \frac{\partial w'}{\partial T_{11}} dT_{11} = dw'. \quad (11.5.10)$$

Then comparison of (11.5.8) and (11.5.10) shows that

$$D_3 = \frac{\partial w'}{\partial E_3}, \quad e_{11} = \frac{\partial w'}{\partial T_{11}}. \quad (11.5.11)$$

It finally follows from this last pair of equations that

$$\frac{\partial D_3}{\partial T_{11}} = \frac{\partial e_{11}}{\partial E_3}, \quad (11.5.12)$$

which is the desired reciprocity condition. The same coefficient γ appears in (11.5.1) and (11.5.3) because the electromechanical coupling is conservative. The following example indicates how these constitutive laws can be the basis for describing the electromechanical dynamics of the bar.

Example 11.5.4. We wish to determine the electrical input admittance to the device shown in Fig. 11.5.7. In this case the electric field intensity E_3 is related to the potential V by

$$E_3 = -\frac{V}{a}. \quad (a)$$

Because E_3 is independent of x , the equation of motion in the bulk of the material does not involve electromechanical coupling; that is, the force equation in the x -direction is

$$\rho \frac{\partial^2 \delta_1}{\partial t^2} = \frac{\partial T_{11}}{\partial x}, \quad (b)$$

and from (11.5.3), in which E_3 is independent of x , this becomes

$$\rho \frac{\partial^2 \delta_1}{\partial t^2} = \frac{1}{S} \frac{\partial^2 \delta_1}{\partial x^2}. \quad (c)$$

The boundary conditions at the free ends of the bar, however, do reflect the effect of the electrical input. It follows from (11.5.3) that because $T_{11}(-c/2, t) = 0$ and $T_{11}(c/2, t) = 0$

$$\frac{\partial \delta_1}{\partial x} \left(\frac{-c}{2}, t \right) = \frac{-\gamma V}{a}, \quad \frac{\partial \delta_1}{\partial x} \left(\frac{c}{2}, t \right) = \frac{-\gamma V}{a} \quad (d)$$

The input admittance is defined as

$$Y = \frac{\hat{I}}{\hat{V}}, \quad V = \operatorname{Re} \hat{V} e^{j\omega t},$$

$$I = \operatorname{Re} \hat{I} e^{j\omega t}, \quad (e)$$

where by conservation of charge on the upper plate

$$\hat{I} = -bj\omega \int_{-c/2}^{c/2} D_3 dx. \quad (f)$$

In view of (11.5.1), (11.5.3), and (a), this expression can also be written as

$$\hat{I} = -j\omega b \int_{-c/2}^{c/2} \left[\frac{\gamma}{S} \frac{d\delta}{dx} - \frac{\epsilon V}{a} (1 - K^2) \right] dx, \quad K^2 = \frac{\gamma^2}{\epsilon S}. \quad (g)$$

To proceed in the computation of the input current we require a knowledge of the distribution of the strain e_{11} over the length c of the transducer, which is obtained by solving the bulk equation (c) subject to boundary conditions (d). Solutions take the form $\delta = \operatorname{Re} \delta(x) \exp j\omega t$, where

$$\delta = A \sin kx + B \cos kx \begin{cases} k = \frac{\omega}{\sqrt{\rho S}}, \\ \delta_1 = \operatorname{Re} \delta(x) e^{j\omega t}. \end{cases} \quad (h)$$

The boundary conditions require that

$$A \cos \left(\frac{kc}{2} \right) + B \sin \left(\frac{kc}{2} \right) = -\frac{\gamma \hat{V}}{ak}, \quad (i)$$

$$A \cos \left(\frac{kc}{2} \right) - B \sin \left(\frac{kc}{2} \right) = -\frac{\gamma \hat{V}}{ak}.$$

These conditions show that $B = 0$ unless $kc/2$ is a multiple of π . In what follows we assume that the driving frequency does not coincide with one of these natural frequencies of the even modes. Only the odd modes are excited by the electrical input. Then by adding the two equations of (i)

$$A = \frac{-\gamma \hat{V}}{ak \cos (kc/2)}. \quad (j)$$

It is now possible to use (h) and (j) to evaluate the current as given in (g). Division of this expression by the voltage \hat{V} gives the required input admittance.

$$Y = j\omega \left(\frac{bc}{a} \right) \epsilon \left[(1 - K^2) + \frac{K^2 \tan (kc/2)}{(kc/2)} \right]. \quad (k)$$

In the absence of piezoelectric coupling the coupling coefficient K is zero and (k) reduces to the admittance of a parallel plate capacitor with a dielectric of permittivity ϵ . Even with the coupling the system appears as a simple capacitance at low frequencies. (Remember that k is proportional to the frequency so that, in the limit in which $\omega \rightarrow 0$, $kc \rightarrow 0$ and the last term in brackets reduces to K^2 .)

As might be expected from the fact that the bar supports elastic waves, there are resonances in the response to a driving potential. The admittance is infinite at frequencies such that $\cos(kc/2) = 0$. For this reason the transducer is often used as a resonator with a single electrical terminal pair. Operation is then limited to frequencies in the neighborhood of one of the infinite admittance points. In this case the electromechanical system can be modeled by the electrical circuit shown in Fig. 11.5.9, which has the admittance

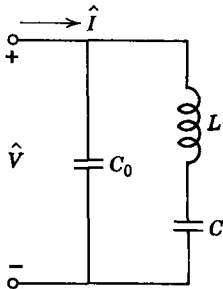


Fig. 11.5.9 Equivalent circuit for expander bar piezoelectric resonator.

$$Y = j\omega \left[C_0 + \frac{1/L}{(1/\sqrt{LC} + \omega)(1/\sqrt{LC} - \omega)} \right], \quad (l)$$

which for ω approximately equal to $1/\sqrt{LC}$ can also be written as

$$Y = j\omega \left[C_0 + \frac{\sqrt{C/L}}{2} \left(\frac{1}{\sqrt{LC}} - \omega \right) \right]. \quad (m)$$

In the neighborhood of the first resonance (k) can be written in this same form by expanding the second term in brackets about the first resonance frequency:

$$\omega = \omega_0 + \omega', \quad \omega_0 = \frac{\pi}{c\sqrt{\rho S}}. \quad (n)$$

Then

$$\frac{kc}{2} \approx \omega_0 \sqrt{\rho S} \frac{c}{2}, \quad (o)$$

$$\cot \left(\frac{kc}{2} \right) \approx -\frac{c}{2} \sqrt{\rho S} \omega',$$

and (k) becomes

$$Y = j\omega \left(\frac{bc}{a} \right) \epsilon \left[(1 - K^2) + \frac{4K^2}{c\pi\sqrt{\rho S}(\omega_0 - \omega)} \right]. \quad (p)$$

Comparison of terms in (m) and (p) shows that the equivalent parameters in the electrical circuit of Fig. 11.5.9 are

$$C_0 = \frac{bc}{a} \epsilon (1 - K^2),$$

$$L = \frac{cS^2 \rho a}{8\gamma^2 b},$$

$$C = \frac{8K^2 \epsilon bc}{a\pi^2}.$$

Of course, even though we have represented the device by an electrical equivalent circuit, it is apparent from the expressions for L and C that the resonance is electromechanical in

nature. The transducer is one way of obtaining an extremely large equivalent L . In practice effects of damping would come into play. The effects of losses would introduce an equivalent resistance into the L - C branch of the equivalent circuit.

The simple piezoelectric resonator discussed in the preceding example can provoke only a small awareness of the wide variety of uses to which piezoelectric phenomena can be put. Much of the attractiveness of the devices based on this interaction is related to their small size and great reliability. Figure 11.5.10 shows a pair of devices that involve the same expander modes as discussed two-dimensionally in the example. Here a thin slab of lead titanate zirconate has several electroded regions, hence constitutes a multi-terminal pair system capable of performing logic and modulator functions. The relative size of the devices is apparent from the figure.

11.6 DISCUSSION

In this chapter we have extended the concepts of Chapters 9 and 10, which were developed by using one-dimensional elastic models, to obtain mathematical models for more complex situations.

This chapter completes our introduction to electromechanical interactions with elastic media. We now proceed to a consideration of electromechanical interactions with fluids.

Fig. 11.5.10 A pair of piezoelectric devices with several electrical terminal pairs. Here the working material is a thin sheet of lead titanate zirconate which undergoes mechanical deformations essentially in the plane of the paper. Note the several electroded regions and the small size. (Courtesy of Sandia Corporation, Albuquerque, New Mexico.)